



UNIVERSITY OF LEEDS

This is a repository copy of *Analytical technology aided optimization and scale-up of impinging jet mixer for reactive crystallization process*.

White Rose Research Online URL for this paper:
<http://eprints.whiterose.ac.uk/81325/>

Version: Accepted Version

Article:

Liu, WJ, Ma, CY, Liu, JJ et al. (2 more authors) (2015) Analytical technology aided optimization and scale-up of impinging jet mixer for reactive crystallization process. *AIChE Journal*, 61 (2). 503 - 517. ISSN 0001-1541

<https://doi.org/10.1002/aic.14662>

Reuse

Unless indicated otherwise, fulltext items are protected by copyright with all rights reserved. The copyright exception in section 29 of the Copyright, Designs and Patents Act 1988 allows the making of a single copy solely for the purpose of non-commercial research or private study within the limits of fair dealing. The publisher or other rights-holder may allow further reproduction and re-use of this version - refer to the White Rose Research Online record for this item. Where records identify the publisher as the copyright holder, users can verify any specific terms of use on the publisher's website.

Takedown

If you consider content in White Rose Research Online to be in breach of UK law, please notify us by emailing eprints@whiterose.ac.uk including the URL of the record and the reason for the withdrawal request.



eprints@whiterose.ac.uk
<https://eprints.whiterose.ac.uk/>

Analytical Technology Aided Optimization and Scale-Up of Impinging Jet Mixer for Reactive Crystallization Process

Wen J. Liu¹, Cai Y. Ma¹, Jing J. Liu^{2,1}, Yang Zhang^{2,1} and Xue Z. Wang^{1,2*}

¹Institute of Particle Science and Engineering, School of Chemical and Process Engineering,
University of Leeds, Leeds LS2 9JT, United Kingdom

²School of Chemistry and Chemical Engineering, South China University of Technology,
Guangzhou 510640, China.

AUTHOR INFORMATION

Wen J. Liu (University of Leeds)

Email pmwliu@leeds.ac.uk

Dr. Cai Y. Ma (University of Leeds)

Email C.Y.Ma@leeds.ac.uk

Dr. Jing Y. Liu (South China University of Technology)

Email: cejjliu@scut.edu.cn

Dr. Yang Zhang (South China University of Technology)

Email: ceyzhang@scut.edu.cn

***Corresponding Author:**

Prof Xue Z. Wang

Chair in Intelligent Measurement and Control

Institute of Particle Science and Engineering

University of Leeds, Leeds LS2 9JT, UK

Tel +44 113 343 2427; Fax +44 113 343 2384; Email x.z.wang@leeds.ac.uk

Notes The authors declare no competing financial interest.

Abstract

Reactive crystallization is widely used in the manufacture of active pharmaceutical ingredients (APIs). Since APIs often have low solubility, traditional stirred tank reactors and the route of process operation and control using metastable zone width are not effective. The current work investigated the integration of an impinging jet mixer and a stirred tank crystallizer that can take advantage of both the reaction and crystallization characteristics, the focus being on design optimization and scale-up using process analytical techniques based on the Fourier transform Infrared spectroscopy and Focused Beam Reflectance Measurement, as well as X-ray diffraction and particle imaging Morphologi G3. The parameters for process operation and design of the impinging jet mixer were optimized. The research was carried out with reference to the manufacture of an antibiotic, sodium cefuroxime, firstly in a 1L reactor, then a 10L reactor. The crystals produced showed higher crystallinity, narrower size distribution, higher stability and purity.

KEYWORDS: Reactive crystallization process; Impinging jet mixer; Process analytical technology; Focused beam reflectance measurement; Sodium cefuroxime

Introduction

Crystallization is widely used in many industries including the pharmaceutical, biopharmaceutical, agrochemical, healthcare, energy, material, food and various personal consumer products. In the pharmaceutical industry, over 80% of all forms of products including tablets, aerosols, capsules, suspensions and suppositories contain crystalline components,¹ making crystallization a very important step of the primary manufacturing stage of pharmaceuticals. The quality of crystals produced is of critical importance since it has a major impact on secondary manufacturing processes such as milling, as well as on the end-use performance, transport and storage of products.^{2,3}

Compared with cooling and anti-solvent crystallization processes, reactive crystallization has been less well studied and understood. Reactive crystallization has many unique features that make it distinctive from cooling or anti-solvent crystallization. The difference even leads to some crystallization concepts and methods not directly applicable to the reactive crystallization process.^{4,5} For instance, the metastable zone width (MSZW) theory may not be applicable because the product generated is often insoluble in the solvent. If the solubility is close to zero, the supersaturation can be near infinity, hence the metastable zone may no longer exist. In addition, under such high supersaturation, in theory secondary nucleation will dominate and be unavoidable. As a result, some researchers have questioned the applicability of the traditional crystal interface growth theory, and proposed new growth mechanisms. For example, some researchers believe that it is the aggregation that dominates the crystal growth during the reactive crystallization processes.⁶⁻⁹

Literature survey reveals that several modelling and experimental studies of reactive crystallization processes, such as the precipitation of L-glutamic acid, have been carried out using traditional crystal interface growth theory.¹⁰⁻¹³ The researchers developed mathematical models

which showed good agreement with the experiments in semi-batch tank crystallizer. However, the growth mechanism may also depend on the solute, solvents, and possibly the mixing conditions and other operating parameters. A major advantage of traditional stirred tank crystallizers is that they are easy to operate and able to produce large particles with low surface area. However, the mixing in such crystallizers is often poor. Therefore, it becomes questionable whether the traditional stirred tank crystallizer is still the favoured process option for reactive crystallization process operating at high supersaturation. The important roles of macro- and micro-mixing in precipitation have been identified by several researchers.^{14,15} The mixing time is not a major concern in the design of a crystallization process when the crystallization kinetic is much slower than the time of mixing.^{16,17} However, for those processes crystallizing very rapidly and/or occurring under high supersaturation conditions, a lack of rapid mixing in the crystallizer can drastically affect the properties of the end product including crystal size distribution, morphology and purity.

As a result, mixing models for reactive crystallization processes have been the subject of studies in the literature.^{18,19} A very promising technique to shorten the mixing time in a reactive crystallizer is a design using jet mixers.²⁰⁻²⁷ In the design, two liquid streams of reactants form narrow, co-planar jets at high velocities impinging upon each other within a small mixing zone. Study on jet mixing as a technique for reactive crystallisation is still limited, in particular for crystallisation of pharmaceuticals. Midler et al^{23,24} tested a jet mixer for rapid precipitation of several pharmaceutical compounds. They found that the mixing intensity in the jet mixer was helpful in rapidly achieving good mixing and a uniformly high supersaturation environment, which led to a high quality final product with superior crystallinity and purity. Mahajan and Kirwan²⁸ reported that the use of a two-impinging-jets precipitator could deliver rapid micromixing and the level of micromixing in the precipitator affected the crystal size distribution of the precipitated product (Lovastatin). By adding a sonication probe close to the impinging

point, Lindrud et al²² produced sub-micron-sized crystals of several pharmaceutical compounds which have great stability and purity. After that, David et al²¹ and Hacherl et al²² proposed that using impinging-jet crystallization could produce a product with desired particle size characteristics. Woo et al^{29,30} also simulated the crystal size distribution in a confined impinging jet crystallizer using the computational fluid dynamics method to provide further understanding of this process. Jiang et al³¹ combined continuous seeding using dual impinging jets with on-line control instruments (ATR-FTIR and FBRM) in a stirred tank and manufactured crystals with a flattop size distribution successfully.

In this study, an impinging jet mixer was designed and integrated with a stirred tank crystallizer for the reactive crystallization process of sodium cefuroxime. The design has taken into consideration the features of both the reaction and the crystallization. A process analytical technique (PAT) using focused beam reflectance measurement (FBRM) was used, together with particle characterization methods using the imaging instrument Morphologi G3 and XRD, to optimize the reaction temperature, feed rate, stirring speed, seed loading, and jet speed, angles and spacing of mixer nozzles. The study was carried out firstly in a 1L vessel, then in a 10L vessel. The ultimate performance was assessed by the product's performance stability and processability.

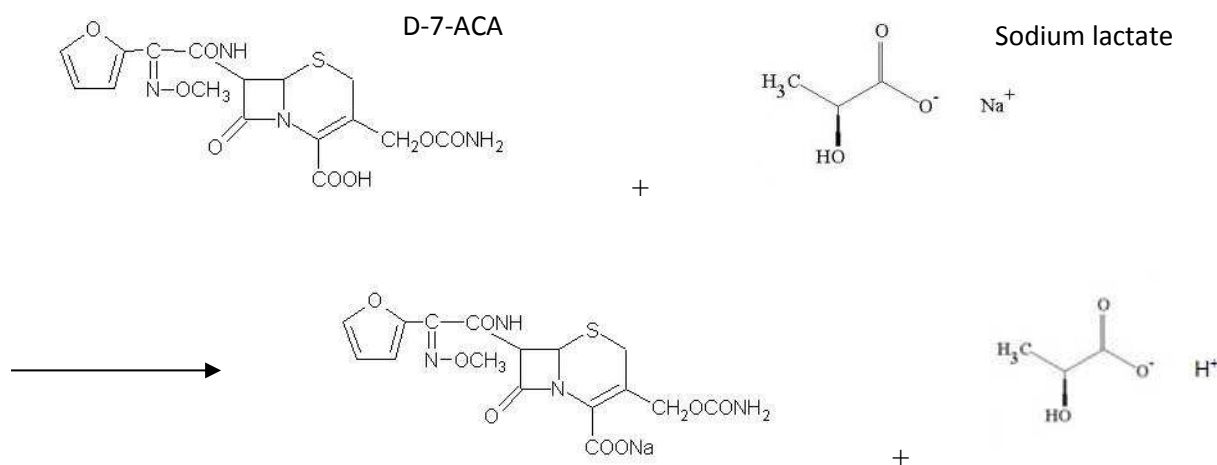
Materials and Experiment

Materials

Cefuroxime is a valuable broad spectrum antibiotic, which has high activity against a wide range of gram-positive and gram-negative micro-organisms.^{32,33} However, its poor stability has been a cause of widespread concern during industrial production. In the storage and transportation processes, it tends to deepen solid colour, reduce solubility and become sticky.³⁴ In our previous paper,³⁰ cefuroxime sodium has only one polymorphic form and exists as a mixture of crystal and

amorphous state. The general view is that the stability of drugs in the amorphous form is usually lower than the crystalline form, because of the higher free energy level under the amorphous form. Therefore, a low degree of crystallinity is one of the main causes resulting in the poor stability of cefuroxime.

In traditional processing methods, 7-ACA (3-(Acetyloxymethyl)-7-amino-8-oxo-5-thia-1-azabicyclo [4.2.0]oct-2-ene-2- carboxylic acid) was used as the reactant. However, 7-ACA needs a strong alkali such as sodium hydroxide to break the acetyl bond which leads to more side reactions, hence affecting product quality. Therefore, a replaced reactant, D-7-ACA (Deacetyl 7-ACA) was used in this study, which is more environmentally-friendly and can further improve the recovery ratio of the product. As a prerequisite work, the solubility of sodium cefuroxime has been measured in our previous study.³⁵ The reaction stoichiometric equation can be seen as follows:



The reaction crystallization process in a stirred tank crystallizer can be described as follows: at first, 9.0 g 60 % w/w sodium lactate aqueous solution (Fisher Scientific UK Ltd) was dissolved in the mixed solvent of 40 mL acetone and 50 mL 95 % ethanol at 20 - 25 °C. The mixture was then filtered and washed with 10 mL 95 % ethanol into a beaker. Next, 10 g acid cefuroxime was dissolved in the mixed solvent of 246 mL acetone and 124 mL 95 % ethanol. The activated

carbon was added in the acid cefuroxime solution and this mixture was stirred for 10 - 15 minutes at 38 - 42 °C, then filtered and the activated carbon needed to be washed with 30 mL acetone. After that, the sodium lactate solution was placed into the tank crystallizer first with 0.03 g sodium cefuroxime crystals added as seeds. Then the acid cefuroxime solution was added into the crystallizer with a feed rate of 4 mL·min⁻¹ at 25 - 28 °C, and the reaction took place immediately at a stirring speed of 80 - 100 rpm. Because sodium cefuroxime is insoluble in the solvent, the solution quickly became turbid. Finally, the reaction products, sodium cefuroxime, needed to be filtered and washed in a mixture of acetone and 95 % ethanol (1.8 : 1) until the pH value reached 8.0. After 24 hours vacuum drying in the DZF-6030B vacuum oven, the final product was obtained. The seeds, sodium cefuroxime crystals (C₁₆H₁₅N₄NaO₈S, 446.37 kg·mol⁻¹, > 92 %, water content < 0.24 %), was produced by an anti-solvent re-crystallization process.³⁵ Ethanol (95% v/v) and activated carbon were obtained from Fisher Scientific UK Ltd, acetone was obtained from Sigma, and the distilled water produced in our own laboratory was also used in this reactive crystallization process.

Methods and Apparatus

Reactive crystallization process

Reactive crystallization of sodium cefuroxime has three main features that have dictated our design of the process: the rapid reaction rate, very low solubility of sodium cefuroxime in the solution, and the high supersaturation as a result of the above two factors. In addition, in the reactor design, other factors also need to be taken into account such as the time scales of crystal growth and reactions, i.e. crystal growth is not as fast a process as the reaction, and crystal growth mechanisms in the process, i.e. the crystal growth is likely to follow an aggregation mechanism rather than a surface growth model or a combination of the two mechanisms. Based on these considerations, a design of a combination of an impinging jet mixer and a stirred tank

crystallizer was proposed and optimized in this study. The impinging jet mixer can achieve high intensity micromixing of fluids so as to form a homogeneous compound prior to the start of nucleation. This technology permits direct crystallization of the high surface area particles with high purity and great stability under high supersaturation, which is favoured by reactive crystallization processes.²¹⁻²³

As mentioned previously, it is believed that both mechanisms, i.e. the seed crystal growth in the supersaturated solution and also aggregate with freshly nucleated material, affect the increase of particle size. In this study, it is assumed that the crystal growth is likely to follow an aggregation mechanism rather than a surface growth model. The injection nozzles should be placed as close as possible to the stirrer of the stirred tank crystallizer, the logic behind this is that the nuclei formed or the small particles can be immediately dispersed in the slurries of the stirred tank crystallizer where crystals are growing. These nuclei or small particles leave the jet nozzle area, then move to the other area in the tank reactor and grow on the surfaces of the existing crystals in that area. The mixture stays in the tank crystallizer for a desirable time period to allow crystals to grow.

The 1L and 10L rigs used for the reactive crystallization process optimization and scale-up are illustrated in Figures 1 and 2. The 1L rig was also used to prepare seeds using the anti-solvent re-crystallization process, by only replacing the focused beam reflectance measurement (FBRM) probe^{36,37} with an attenuated total reflectance-Fourier transform infrared (ATR-FTIR) probe.³⁸ In the anti-solvent re-crystallization process, ATR-FTIR was used for monitoring the supersaturation. In the reactive crystallization process, FBRM was used to monitor crystallization processes and to provide qualitative and quantitative information about nucleation and crystal growth.^{39,40}

The 1L and 10L tank reactors are both cylindrical in shape with a jacket to control the reaction temperature by water/oil circulation. The 1L and 10L vessels are not baffled. The diameter and height of the 1L reactor are 10 cm and 12 cm, respectively. The impeller in the 1L reactor is 45° pitched blade impeller with a diameter and height of 5 cm and 2 cm, respectively. The diameter and height of the 10L reactor are 20 cm and 30 cm, respectively. The impeller in the 10L reactor is a radial-flow blade turbine impeller with a diameter and height of 14 cm and 5.5 cm, respectively.

Pressure drop

In the design of an impinging jet mixer probe, the pressure drop is the main parameter for the selection of the pump and the determination of the nozzle diameter.⁴¹ The pressure drop is composed of pipe friction pressure drop, static pressure drop and velocity pressure drop. The formula is as follows:

$$\Delta P = \rho g(Z_2 - Z_1)10^{-3} + \rho \frac{(u_2^2 - u_1^2)}{2} 10^{-3} + \rho \sum h_f 10^{-3} \quad (1)$$

$$\sum h_f = \lambda \frac{(L + \sum L_e) u^2}{D} \quad (2)$$

or

$$\Delta P = \Delta P_S + \Delta P_N + \Delta P_f \quad (3)$$

where ΔP is the total pressure drop of the piping system, kPa; ΔP_S is the static pressure drop, kPa; ΔP_N is the velocity pressure drop, kPa; ΔP_f is the friction pressure drop, kPa; Z_1 is the height of the beginning of the pipeline, m; Z_2 is the height of the ending of the pipeline, m; g is the gravity acceleration, $9.81 \text{ m}\cdot\text{s}^{-2}$; u_1 is the fluid flow rate of the pipeline beginning, $\text{m}\cdot\text{s}^{-1}$; u_2 is the fluid flow rate of the pipeline ending, $\text{m}\cdot\text{s}^{-1}$; ρ is the fluid density, $\text{kg}\cdot\text{m}^{-3}$; h_f is the friction energy loss,

$\text{J}\cdot\text{kg}^{-1}$; L is the pipe length, m; L_e is the equivalent length of fittings, m, and D is the pipe inner diameter, m.

The flow pattern in the pipeline also has a significant impact on the pressure drop. The flow pattern involves the laminar flow and the turbulent flow, the criteria for determining the fluid flow pattern is the Reynolds number. The formula is as follows:

$$Re = \frac{Du\rho}{\mu} \quad (4)$$

where Re is the Reynolds number and μ is fluid viscosity, $\text{mPa}\cdot\text{s}$.

The friction coefficient (λ) in Eq. (2) is a function of the Reynolds number and the pipe relative roughness. The formula is as follows:

$$\lambda = \frac{64}{Re} \quad (5)$$

The formula of pipe friction pressure drop is as follows:

$$\Delta P_f = \frac{32\mu u L}{D^2} \quad (6)$$

The formula of the static pressure drop is as follows:

$$\Delta P_s = \rho g(Z_2 - Z_1)10^{-3} \quad (7)$$

The formula of the velocity pressure drop is as follows:

$$\Delta P_N = \rho \frac{(u_2^2 - u_1^2)}{2} 10^{-3} \quad (8)$$

According to the desired flow rate, the diameters of the two nozzles were 0.13 mm and 0.065 mm in the 1L crystallizer, 0.3 mm and 0.15 mm in the 10L crystallizer, and the theoretical pressure drops in the tubes with an identical tube length of 500 mm were roughly 9.5 MPa and 38 MPa in the 1L crystallizer, 1.8 MPa and 7.1 MPa in the 10L crystallizer, respectively. To meet the

required high pressure drops and also the flow rates, the 307 Piston Pump with a high pressure limit of 60 MPa was selected.

Analytical characterization

X-ray diffraction data was collected using a Bruker D8 advance (CuK α 1, $\lambda = 1.540598\text{\AA}$). Yttria (Y₂O₃) was used as standard for the estimation of instrumental peak broadening. The size distribution data were collected using the Morphologi G3 Particle Size and Particle Shape Analyzer from Malvern. The Morphologi G3 measures the size and shape of particles using the technique of static image analysis. Fully automation with integrated dry sample preparation makes it the ideal replacement for costly and time-consuming manual microscopy measurements. After 24 hours vacuum drying in the vacuum oven, the same amount of samples was used for each XRD measurement and Morphologi G3 analysis. Colour grade data were obtained by drug accelerated test using a stability chamber (Labonce-60GS) and a UV instrument (SHIMADZU UVmini-1240) was used to determine the transmittance.

The detailed operation of the stability test in this study was as follows: the sealed sodium cefuroxime samples were placed in the stability chamber under 40 °C/60 °C without light. After a fixed number of days (3 days, 5 days, 7 days and 10 days), 0.6 g sample was taken and dissolved in 5 mL distilled water, and then compared with the standard solution to decide the colour grade level by use of a UV instrument. The standard solution has ten colour levels with the lower level indicating the better stability and longer shelf-life.

Results and Discussion

The original operation for industrial application of sodium cefuroxime synthesis process was: putting the sodium lactate solution in the reactor first with 0.03 g sodium cefuroxime added as seeds, the acid cefuroxime solution was added to the reactor with 4 - 6 mL·min⁻¹ feed rate at 25 -

28 °C, and the reaction took place immediately on stirring. Therefore, the main parameters in this study are: the reaction temperature, the feed rate, the stirring speed and the amount of seeds. In this section, the optimization experiments of operation parameters were carried out firstly in the 1L tank reactor without the impinging jet mixer (Table 1). Then, the optimization experiments of the impinging jet mixer were also carried out in the 1L tank reactor based on the optimized operation parameters obtained already. Finally, the 10L impinging jet mixer scale-up experiments were carried out to further verify this novel impinging jet mixer design.

In this study, increasing the crystallinity of the product, hence improving the stability, was the main purpose. As the XRD spectra are directly relevant to the perfection level of crystal structure, the spectra results were used to judge the crystallinity. This is attributed to the fact that our product exists as a mixture of crystal and amorphous state. Furthermore, comparing with the stability test (3 days, 5 days, 7 days and 10 days), XRD spectra can be measured quickly and gives direct evidence of the process optimization. Three sharp peaks of the XRD spectra of sodium cefuroxime were observed at 2θ values of 9° to 10.5° , 10.5° to 13° and 14° to 15° .³⁰ The peak intensity and peak width at half height of peak between 9° to 10.5° were chosen to present the crystallinity of sodium cefuroxime for quantification in this study. The products obtained from the 1L and 10L crystallizers were used to perform the stability measurement and the HPLC test for purity.

Optimization of Operating Conditions

Reaction temperature

At a higher temperature, the increasing Brownian motion can make the dispersion rate of a solute in a solvent much larger than that at a lower temperature. Therefore, high temperature conditions can promote the forward reaction. If the other conditions are kept the same, the time required to reach equilibrium is inversely proportional to the temperature increase, i.e. as the temperature

increases, the time spent on reaching equilibrium can be rapidly shortened. As a result, it seems that when possible, a higher reaction temperature should be used during a reaction process. However, at the same time, the reaction temperature is also one of the important factors that can affect the quality of the final product; in particular, the impact on the product colour grade is very significant. Sodium cefuroxime is known as a kind of β -lactam antibiotic,³⁰ which has ester and amide functional groups within its molecular structure. This means that the hydrolysis of the ester and amide bonds become the main factor in causing chemical degradation. Under higher temperature, this chemical degradation can be more severe, hence resulting in lower product stability. In our studies, it was found that the mother liquor colour grade at the end of the reaction could become yellower, even by visual observation, after filtration if the reaction temperature was too high. In addition, the product obtained from higher temperature reaction was often caked or hardened, which was not conducive to the drying and milling processes.⁴²

In order to investigate the influence of reaction temperature on the crystallization process, the test reaction temperatures were 20 °C (AEIN), 25 °C (BFIN), 30 °C (CFIN), and 35 °C (DFIN). The XRD spectra results (Figure 3(a)) showed that the reaction temperature within the tested temperature range had little effect on the crystalline state. Therefore, the optimization tests were performed at room temperature (20 - 25 °C).

Feed rate

For the reactive process, the feed rate had a direct impact on the reaction rate. Generally, a very fast feed rate would make the reactants react insufficiently, hence leading to the final products mixing with the unreacted reactants. For the crystallization process, a fast feed rate would make local supersaturation increase rapidly, in particular, in larger-scale crystallizers, which is more likely to cause non-uniform supersaturation distribution, hence resulting in low crystallinity of

the product. On the contrary, a slow feed rate is conducive to the growth of crystals, but it might not be a desirable operating condition because it would lengthen the production time.

On the basis of the industrial feed time, several test feed rates were used in the current studies: 2 mL·min⁻¹ (BEIN), 4 mL·min⁻¹ (BFIN), 6 mL·min⁻¹ (BGIN) and 8 mL·min⁻¹ (BHIN). The XRD spectra results (Figure 3(b)) showed that the feed rates of 2 mL·min⁻¹ and 4 mL·min⁻¹ produced crystals with a higher crystallinity, which meant that the slow feed rate was more conducive for sodium cefuroxime crystalline formation.

Stirring speed

In a crystallization process, stirring can keep the solution concentration in a more uniform state, hence leading to the corresponding supersaturation on the crystal interface being more uniform. The use of stirring can also cause the crystals to collide with each other and to influence the local environment and temperature distributions for the crystals to grow. However, a higher stirring speed also produces large horizontal shear force, which can break the formed crystals. Therefore, the determination of a suitable stirring speed is one of the necessary conditions for producing high quality crystals from reactive crystallization processes under the current investigation.

On the basis of the industrial operating parameters, the tested stirring speeds were: 80 rpm (BFIN), 100 rpm (BFJN), 150 rpm (BFKN) and 200 rpm (BFLN). The XRD spectra results (Figure 3(c)) showed that an appropriate stirring speed within a range of 80 - 100 rpm provided proper collision opportunities for crystal growth and also maintained the solution concentration uniformity. The Morphologi G3 results also showed that an appropriate stirring speed (such as 80 -100 rpm) was able to produce narrower particle size distribution (Figure 4). However, if the stirring speed was set too high (such as 150 - 200 rpm), the crystals subjected to greater shear force would be broken into small particles, hence not only resulting in the number of particles being increased, but also leading to more amorphous particles in the final products. The

Morphologi G3 results (Figure 4) indicate that the fluid stresses are sufficient to break the crystal that grew following an aggregation mechanism. This may be the main cause for a bi-modal CSD.

In addition, there were still two noteworthy issues: a) for the reactive crystallization process, sufficient mixing of the reactants was conducive to the reaction procedure and helpful in keeping the uniform distribution of supersaturation at the same time. Generally, it was believed that increasing the stirring speed could make mixing better, but for some relatively fragile crystals, a higher stirring speed would break the crystals with higher possibilities. b) the optimum stirring speed was only targeted with the laboratory crystallizer configurations and the type of stirring paddle used in the current study. If the crystallizer configuration or the paddle type is changed, the similar procedure can be used to obtain the corresponding optimum stirring speed.

Amount of seeds

Different amounts of seed results in different final products. Too few seeds will not help to suppress the secondary nucleation, while too many seeds may lead to the formation of tiny crystals. A simplified method was generally used to estimate the appropriate amount of seeds in the industry.⁴³ The load of the seed can be predicted from the amount of the solute dissolved in the solvent, the size of the seed and the desired size of the final product. A crystallization process that has only crystal growth and the formation of nuclei can be ignored, the number of product crystals should be equal to the number of seeded crystals as described in the following formula,

$$\frac{M_P}{K_V \rho V_P} = \frac{M_S}{K_V \rho V_S} \quad (9)$$

where M_p and M_s are the mass of the product crystals and the seed crystals, respectively, g; K_v is the volume shape factor; V_p and V_s are the average volume of the product crystals and the seed crystals, respectively.

Obviously, this is only a simplified approach. The expression of the average size of the product crystals and seeded crystals is far less accurate. For almost all of the crystallization processes, secondary nucleation is inevitable. However, this approach can provide a reference for further research. Using this method, the optimal amount of seeds required was found to be 0.03 g in the current study.

To further confirm the amount of seeds, FBRM (Focused Beam Reflectance Measurement, LASENTEC, S400A Controller, PI-14/206 PROBE) was used in the un-seeded reaction. As the FBRM could detect and count the number of crystals in the crystallizer,^{44,45} the plan was to select a quick initial feed rate to produce different numbers of seeds, and then slow down the feed rate to avoid secondary nucleation. Two different initial feed rates, 4 mL·min⁻¹ (20120523) and 10 mL·min⁻¹ (20120524) were selected, corresponding to the slower and faster feed rates respectively. In order to prevent excessive feeding which would lead to the generation of too many seed crystals, the feed pump was opened one minute in every five minutes. The feed rate was changed only in the experiments for the determination of the amount of seeds. In other experiments either for operating parameter optimization or for impinging jet design, the feed pump operated during the entire reactive crystallization process with the optimized feed rate of 4 mL·min⁻¹ for the reactant feed.

Faster feeding can produce a larger number of crystals. Therefore, in our study, the faster feeding was only used for a higher degree of supersaturation to ensure different amounts of seeds can be generated quickly at the very beginning of the entire reactive crystallization process. After that, a slower feeding was used to reduce the degree of supersaturation to inhibit secondary nucleation. Besides, the presence of an appropriate number of seeds can also lower the degree of supersaturation in the solution which could further inhibit secondary nucleation. Here, secondary nucleation means the nucleation that occurred after the seeds were added.

The results given in Figure 5(a) and (b) showed that when the feeding amount reached 40 mL - 70 mL, the seed crystals generated could obviously be detected. The number of each crystal size generated by faster initial feeding rate was significantly less than that generated by a slower initial rate, which meant that the faster initial rate quickly made enough seeds to suppress secondary nucleation. The final total count was 35,000 and 25,000, respectively. It also revealed that in the case of a certain amount of product, the crystal size obtained with the faster initial feed rate ($10 \text{ mL}\cdot\text{min}^{-1}$) was bigger than that with the slower one ($4 \text{ mL}\cdot\text{min}^{-1}$) because of the lower total count, which could make the filtration process more easily and quickly. Two repeat experiments were then conducted following the same conditions with 20120523 and 20120524, respectively. The results in Figure 5(c) showed that when using $10 \text{ mL}\cdot\text{min}^{-1}$ as the initial feed rate (20120524), the growth rate of the total count was significantly slower during the time period between 50 – 90 minutes, which further confirmed that the appropriate number of seeds can inhibit the secondary nucleation during the reactive crystallization process, hence confining the nucleation process and promoting the growth process.

The un-seeded tests demonstrated the influence of the initial amount of seed crystals on the final product (Figure 6). As can be seen from the FBRM result (Figure 5(c)) and XRD spectra results, if the feed rate was changed from $10 \text{ mL}\cdot\text{min}^{-1}$ to $4 \text{ mL}\cdot\text{min}^{-1}$ when the total count reached 5000, the crystallinity of the product was better. Therefore, in order to get the appropriate amount of seeds in the following experiments, the seeds obtained from the anti-solvent re-crystallization method were added into the crystallizer directly and the reactant feed only began when the total count reached 3000 - 5000, then the change of the weight was weighed to obtain the optimum amount of seeds. When using this method, the seed obtained using the anti-solvent re-crystallization method was assumed to be the same as the seeds produced by itself at the beginning of the reactive crystallization process, because it is difficult to obtain the profile of the seeds produced using faster feeding rate at the beginning of the reactive crystallization when the

FBRM counts reach 5000 #/s. Two repeat experiments were carried out to further verify that the seed amount obtain from this replacement process (using the seeds obtained from anti-solvent re-crystallization to replace the seeds produced by the reaction itself) under this assumption can produce a high quality product.

As can be seen from the results of the seeded tests (Figure 7), the total count was kept below 30000 in all cases, and the optimal seed amount by the weighing method was 0.407 g. Compared with 0.03 g of seeds calculated by Eq. (9) in the previous discussion, this big difference in the amount of seeds showed that secondary nucleation phenomena cannot be ignored in reaction crystallization processes of sodium cefuroxime. In fact, for such a rapid crystallization process, it was difficult to completely avoid secondary nucleation phenomena. Even manipulating and optimizing the amount of seeds to be used can only play a supporting role.

Design of impinging jet mixer nozzles

Midler et al²³ suggested that the nozzles of the impinging jet mixer could have a slight downward angle of about 10° from the horizontal to help the flowing material move down and the linear velocity at the jet nozzles should be at least $5 \text{ m}\cdot\text{s}^{-1}$ with the most preferable one being between about 20 to $25 \text{ m}\cdot\text{s}^{-1}$. However, there was no data or experimental results given to support the selection. Jiang et al³¹ inserted needles into a standard plastic Y-mixer for a dual impinging jets configuration but did not provide parameter details of the jet nozzles. For different reactive crystallization processes, these structural parameters obviously might be varied slightly. Therefore, it is necessary to investigate the impact of design parameters of the impinging jet mixer on crystal structure of the product in the current study. To decide the best angle and spacing of the nozzles, three angles and two spaces (6.78 mm, 11.76 mm) were chosen as shown in Table 2. Taking into account the working range of the pumps, the feed speeds of $10 \text{ m}\cdot\text{s}^{-1}$, $15 \text{ m}\cdot\text{s}^{-1}$, $20 \text{ m}\cdot\text{s}^{-1}$ were selected as the feeding speed tests (Table 2).

10° upward jets

The nozzle arrangements of 10° upward jets were tested in this study with two spacing distances. As can be seen from Figure 8(a), from an overall point of view, the product crystallinity with a wider spacing was higher than the narrow one. This might be due to the fact that the wider spacing increased the location of the collision point of the two fluids, hence resulting in more liquid to have the opportunity to collide with the upper part of the mixer probe and then mix with each other when flowing downward. Furthermore, regardless of the spacing size, basically, the product with a slower feed speed had a better degree of crystallinity, and the seeded case was better than the un-seeded one.

Parallel jets

Parallel jets were introduced by many researchers in the literature, and also used in many experimental processes.^{21,22,30} Theoretically, this feed method can guarantee the two jet fluids to have a frontal collision with their maximum speeds, hence possibly resulting in the best mixing effectiveness. However, for the synthesis process of sodium cefuroxime or other drugs, the biggest drawback of this jet configuration is that the parallel jets can very easily cause product accumulation at the outlet of a nozzle of smaller diameter. The main reason was that the two jets did not have equal feed amounts of the two fluids in this study. Since the feed volume ratio of the two fluids was 1:4 (sodium lactate solution: acid cefuroxime solution), at the same feed speed, the momentum of the smaller amount of fluid feed was half of the larger one, which caused the collision point of two jet streams gradually to be moved to the tube outlet of the fluid with a smaller diameter and a lesser amount of feed (the tube for feed sodium lactate solution), eventually leading to the product accumulating slowly at this tube outlet.

The XRD results of the products obtained from the parallel jets configuration were almost the same as those obtained with the 10° upward jets (Figure 8(b)). The crystallization process with

wide spacing produced almost identical product crystallinity when the process had a narrow spacing. For parallel jets, the impact of mixing was only related to the feed speed, so in the case of a high feed speed, the change in spacing had little effect on the experimental results. Furthermore, the product with the slower feed speed also had a better degree of crystallinity and the seeded case was, again, better than the un-seeded one.

10° downward jets

In our study, the clogging could sometimes be observed in the experiments of both 10° upward jets and parallel jets. When the jets were partially clogged, the reactants might just enter into the reactor for reaction without face to face collision similar to how they reacted in the conventional tank reactor.

To avoid clogging, a design with 10° downward feed jets was selected in most of the literature.⁴⁶⁻

⁴⁹ This feed method can avoid the two fluids from direct frontal collision. Although the collision rate would decline, when the momentum difference between the two fluids was large, it could avoid one fluid stream pushing the collision point of the two streams to the other stream.

The XRD results with 10° downward jets were better than those with the 10° upward and parallel jets (Figure 8(c)). The product crystallinity of crystals obtained with a narrow spacing was better than that with the wide one. This may be due to the jets being submerged in the liquid, thus the wide spacing might cause the encountering speeds of the two fluids to be decreased because of the liquid resistance in the crystallizer. This feed method was neither like the 10° upward jets that had the upper part of the mixer probe for collision to increase mixing, nor like the parallel jets that provided a frontal collision. Therefore, the collision effect had a significant effect on mixing effectiveness. Meanwhile, the product with a slower feed speed still had a better degree of crystallinity and the seeded case was still better than the un-seeded one.

Product characterization

After the above optimization experiments in the 1L tank reactor, the optimized operating conditions were:

- Temperature: 20 - 25 °C
- The feed rate: 4 mL·min⁻¹ for acid cefuroxime solution and 1 mL·min⁻¹ for sodium lactate solution
- The stirring speed: 80 - 100 rpm
- Seeds: 0.407 g
- Feeding speed: 10 m·s⁻¹
- Probe (0.13 mm and 0.065 mm): 10° downward jets with 6.78 mm spacing

These optimized operating conditions were used to do three repeated tests (1L with impinging jet mixer, re-1L with impinging jet mixer-1 and re-1L with impinging jet mixer-2). The XRD spectra (Figure 9) showed the improvement of the crystallinity of the product. As can be seen from the results of the Morphologi G3 (Figure 10), compared with the product obtained using the same operating conditions without the impinging jet mixer (1L without impinging jet mixer), the size distributions were narrower.

As mentioned in the literature,^{28,50} a high linear velocity could produce crystals with higher crystallinity. However, our conclusion was that a slower feed speed was a better choice for obtaining crystals with higher crystallinity, which might be because that the mechanism of sodium cefuroxime crystal growth being different. Several theories have been proposed to explain the mechanism of crystal growth.⁵¹ The diffusion-reaction theory suggested that once an ordered crystal structure is formed by nucleation, the growth units (atoms, ions or molecules) can diffuse from the surrounding supersaturated solution to the surface of the nucleus and result in crystal growth. Based on the adsorption layer theory, particle growth occurs on pre-existing

layers of atoms or molecules that adsorbed on crystal faces. Besides these theories, another phenomenon which causes the size to increase is aggregation.^{5,52} Solution hydrodynamics, static forces, and particle structures may all have effects on crystal aggregation. Meanwhile, aggregation can mainly occur in supersaturated solutions as it requires high levels of supersaturation to build the bonding between particles.

The sodium cefuroxime synthesis process, the combination of the reaction process and the crystallization process, is such a process which conducts under high levels of supersaturation. The huge supersaturation was firstly generated by the reaction because the product cannot be dissolved in solvents completely, then the nuclei were generated and, further, the growth process occurred when the nuclei met the crystal seeds in the crystallizer. Besides the competition between the nucleation process and the growth process during this crystallization process, the kinetic of the reaction itself also directly affects the whole process by varying the supersaturation. In a traditional stirred tank crystallizer, the nucleation and growth processes were carried out at the same time and in the same place. The impinging jet mixer in this study was designed to avoid the simultaneous existence of the nucleation and growth processes by confining the nucleation and growth processes within the corresponding nucleation area and growth areas. In the nucleation area, the novel impinging jet mixer was used to achieve complete mixing of reactants for reaction and to generate small nuclei. Then the impeller drove these small nuclei from the nucleation area to the growth area where the nuclei contact with the crystal seeds in the crystallizer for growth.

A very fast feed speed could force the two reactants to leave the nucleation area and enter the growth area before sufficient reaction had occurred, which leads to both the nucleation and growth processes taking place in the same place just like the conventional crystallizers. Obviously, in order to use this newly-devised impinging jet mixer probe for obtaining high quality crystals, the selection of a suitable feed speed is very important. Both the mixing

effectiveness and the reaction kinetics should be considered. As long as it ensured that the reaction could be finished in the nucleation area, the faster the feed speed was, the better the product crystallinity obtained.

In addition, we also tested the configuration with the impinging jets being located above the liquid level of the stirred tank crystallizer, but unlike the findings of Hacherl et al²² for the calcium oxalate modelling system, the crystallinity of the product obtained was not satisfactory which might be because without the solvent resistance to the jet streams, the feed speed was too high to produce sufficient reaction.

Impinging jet mixer scale-up in the 10L vessel

In order to achieve industrialization, the scale-up process becomes one of the important final steps. Scale-up is to use the successfully optimized process in the laboratory small-scale reactor under industrial production conditions to verify the feasibility of this original process after amplification of reactor size, capacity, etc. and to ensure the consistency of the processes. Therefore the scale-up process studied can verify, review and improve the laboratory process results and provide reliable production data, as well as the material quality and consumption for industrial production, it can also resolve problems which have not been solved or have not yet been discovered at the laboratory stage.

The instruments for the 10L scale-up can be seen in Figure 2. Since a single pump cannot reach the required feed rate, three pumps were used and joined forces for the acid cefuroxime solution feeding. At the beginning, the scale-up was based on the same feed velocity ($10 \text{ m}\cdot\text{s}^{-1}$) as in the 1L crystallizer with a volumetric scaling-up factor of 10 while keeping all other operation parameters the same. The 10L scale-up experiments were conducted at room temperature and the parameters were as follows:

- Temperature: 20 - 25 °C
- The feed rate: 40 mL·min⁻¹ for acid cefuroxime solution and 10 mL·min⁻¹ for sodium lactate solution
- The stirring speed: 80 - 100 rpm
- Seeds: 4.07 g
- Feeding speed: 10 m·s⁻¹
- Probe (0.3 mm and 0.15 mm): 10⁰ downward jets with 6.78 mm spacing.

Followed the above operating conditions, the crystal size distribution (10L with impinging jet mixer-80 rpm) was not satisfied (Figure 11 and Figure 12). Based on the conclusions obtained from the optimization experiment of the 1L tank reactor that the stirring speed affects the crystal size distribution, a reduced stirring speed of 50 rpm was used to increase the residence time of the reactants in the nucleation area. With the reduced stirring speed, the results from the test experiment (10L with impinging jet mixer-50 rpm) showed narrower crystal size distribution. Then the test experiment (re-10L with impinging jet mixer-50 rpm) was carried out and satisfactory results were obtained (Figure 11 and Figure 12). Compared with the product obtained using the same operating conditions without the impinging jet mixer (10L without impinging jet mixer-50 rpm), the size distribution became narrower. The XRD spectra (Figure 11) showed improvement in the crystallinity of the product. The SEM results in Figure 13 showed that the product obtained with the impinging jet mixer (Figure 13 (b)) had an almost similar level of aggregation with the seeds (Figure 13 (c)) while the product obtained without the impinging jet mixer (Figure 13 (a)) had more severe aggregation than the seeds.

Product analytical profile

From Table 3 and Table 5, it can be seen that the products obtained with the impinging jet mixer probe, compared with the comparative one obtained without the impinging jet mixer probe (1L

without impinging jet mixer and 10L without impinging jet mixer-50 rpm), had lower water and impurity content. It verified that the crystallinity was improved by using this new feed mode. Better crystal structure, besides reducing the defect of the crystal, could reduce the possibility of the moisture and impurities being wrapped in crystals during the crystal growth process.

As can be seen from the stability results (Table 4 and Table 6), under the condition of 40 °C, the colour grade levels obtained from the 10L scale-up samples were almost the same, which was one level lower than the comparative one (10L without impinging jet mixer-50 rpm). Under the condition of 60 °C, the colour grades obtained in both the 1L and 10L crystallizer with the impinging jet mixer probe were at least two levels lower than the comparative one (lower colour grade means more stability of the product).

Conclusions

Reactive crystallization of sodium cefuroxime was examined and found to have three main features: rapid reaction, very low solubility of sodium cefuroxime in the solvent, and as a result huge supersaturation. Based on the mechanistic understanding, the process was designed to have an impinging jet mixer submerged in the solution of a stirred tank crystallizer, placing the jet nozzles as close as possible to the stirrer. The thinking was that the impinging jet mixer achieves high intensity micromixing of fluids so as to form a homogeneous compound prior to the start of nucleation, and that the formed nuclei or the small particles are immediately dispersed in the slurries of the stirred tank crystallizer where crystals are growing so that these nuclei or small particles leaving the jet nozzles will move to, and grow on the surfaces of the growing crystals, rather than the nuclei and small particles themselves further aggregate. The stirred tank crystallizer allows the mixture to have sufficient residence time in the tank to undergo growing to grow (or aggregates) to larger high quality crystals.

Focused beam reflectance measurement (FBRM) was used to optimize the process design parameters and operating conditions including reaction temperature, feed rate, stirring speed, and seed loading. The optimized operating parameters were: 20 – 25 °C for reaction temperature, 4 mL·min⁻¹ for feeding rate, 80 – 100 rpm for stirring speed, and 0.407 g for the amount of seeds in the 1L crystallizer; 20 – 25 °C for reaction temperature, 4 mL·min⁻¹ for feeding rate, 50 rpm for stirring speed, and 4.07 g for the amount of seeds in the 10L crystallizer. The feed speed, angle and spacing of nozzles were also optimised based on the performance of the product. The diameters of the two nozzles were 0.13 mm and 0.065 mm in the 1L crystallizer, 0.3 mm and 0.15 mm in the 10L crystallizer. The experimental results indicated that both 1L and 10L crystallizers provided high quality products. Both 1L and 10L crystallizers produced crystals of higher crystallinity (XRD spectra), narrower size distribution (Morphologi G3), higher stability (stability test), and purity (HPLC).

List of Abbreviations

API	Active pharmaceutical ingredient
MSZW	Metastable zone width
PAT	Process analytical technology
ATR-FTIR	Attenuated total reflectance-Fourier transform infrared
FBRM	Focused beam reflectance measurement
XRD	X-ray diffraction

Acknowledgments

Financial Support from UK Engineering and Physical Sciences Research Council (EP/H008012/1, EP/H008853/1), China Scholarship Council (CSC), and funding of the China One Thousand Talents Scheme are gratefully acknowledged.

Literature Cited

1. Shekunov BY, York P. Crystallization processes in pharmaceutical technology and drug delivery design. *Journal of Crystal Growth*. 2000;211(1-4):122-136.
2. Desikan S, Anderson SR, Meenan PA, Toma PH. Crystallization challenges in drug development: scale-up from laboratory to pilot plant and beyond. *Current opinion in drug discovery & development*. 2000 2000;3(6):723-733.
3. Shan G, Igarashi K, Noda H, Ooshima H. Control of solvent-mediated transformation of crystal polymorphs using a newly developed batch crystallizer (WWDJ-crystallizer). *Chemical Engineering Journal*. 28 2002;85(2-3):169-176.
4. Chen M, Ma CY, Mahmud T, Darr JA, Wang XZ. Modelling and simulation of continuous hydrothermal flow synthesis process for nano-materials manufacture. *Journal of Supercritical Fluids*. 2011;59:131-139.
5. Lu J, Wang JK. Agglomeration, breakage, population balance, and crystallization kinetics of reactive precipitation process. *Chemical Engineering Communications*. 2006;193(7):891-902.
6. Ma CY, Chen M, Wang XZ. Modelling and simulation of counter-current and confined-jet reactors for hydrothermal synthesis of nano-materials. *Chemical Engineering Science* 2014;109:26-37.
7. Erriguible A, Mariasi F, Cansell F, Aymonier C. Monodisperse model to predict the growth of inorganic nanostructured particles in supercritical fluids through a coalescence and aggregation mechanism. *Journal of Supercritical Fluids*. 2009;48(1):79-84.
8. Alonso E, Montequi I, Lucas S, Cocero MJ. Synthesis of titanium oxide particles in supercritical CO₂: Effect of operational variables in the characteristics of the final product. *Journal of Supercritical Fluids*. 2007;39(3):453-461.
9. Peukert W, Schwarzer HC, Stenger F. Control of aggregation in production and handling of nanoparticles. *Chemical Engineering and Processing*. 2005;44(2):245-252.
10. Alatalo H, Hatakka H, Kohonen J, Reinikainen S-p, Louhi-kultanen M. Process Control and Monitoring of Reactive Crystallization of L-Glutamic Acid. *Aiche Journal*. 2010;56(8):2063-2076.

11. Borissova A, Jammoal Y, Javed KH, et al. Modeling the precipitation of L-glutamic acid via acidification of monosodium glutamate. *Crystal Growth & Design*. 2005;5(3):845-854.
12. Scholl J, Vicum L, Muller M, Mazzotti M. Precipitation of L-glutamic acid: Determination of nucleation kinetics. *Chemical Engineering & Technology*. 2006;29(2):257-264.
13. Su QL, Chiu MS, Braatz RD. Modeling and Bayesian Parameter Estimation for Semibatch pH-Shift Reactive Crystallization of L-Glutamic Acid. *Aiche Journal*. 2014;60(8):2828-2838.
14. Chen JF, Zheng C, Chen GT. Interaction of macro- and micromixing on particle size distribution in reactive precipitation. *Chemical Engineering Science*. 1996;51(10):1957-1966.
15. Judat B, Racina A, Kind M. Macro- and micromixing in a Taylor-Couette reactor with axial flow and their influence on the precipitation of barium sulfate. *Chemical Engineering & Technology*. 2004;27(3):287-292.
16. Coker EN, Dixon AG, Thompson RW, Sacco A. Zeolite synthesis in unstirred batch reactors .3. effect of nonuniform pre-mixing on the crystallization of zeolite-a and zeolite-x. *Microporous Materials*. 1995;3(6):637-646.
17. Goronszy MC, Rigel D. Biological phosphorus removal in a fed-batch reactor without anoxic mixing sequences. *Research Journal of the Water Pollution Control Federation*. 1991;63(3):248-258.
18. Garside J, Tavare NS. Mixing, reaction and precipitation - limits of micromixing in an msmpr crystallizer. *Chemical Engineering Science*. 1985;40(8):1485-1493.
19. Pohorecki R, Baldyga J. The use of a new model of micromixing for determination of crystal size in precipitation. *Chemical Engineering Science*. 1983;38(1):79-83.
20. Tamir A, Kitron A. Applications of impinging-streams in chemical-engineering processes - review. *Chemical Engineering Communications*. 1987;50(1-6):241-330.
21. David, Thomas C. Crawford, Weston NP, Inventors. Reactive crystallization method to improve particle size. US 6,558,435 B2. 2003.
22. Lindrud MD, Kim S, Wei C, Inventors. Sonic impinging jet crystallization apparatus and process. US 6,302,958 B1. 2001.
23. Midler M, Paul EL, Whittington EF, et al., Inventors. Crystallization method to improve crystal structure and size. US 5,314,506. 1994.
24. Midler M, E. L. Paul, Whittington EF. Production of high purity, high surface area crystalline solids by turbulent contacting and controlled secondary nucleation. *Engineering Foundation Conf. on Mixing, Potosi, Mo*. 1989.
25. Liu PD, M. Futran, M. Midler, Paul EL. Particle size design of pharmaceuticals by continuously impinging jets precipitation. *AICHe Meeting, Chicago*. 1990.
26. Hacherl JM, Paul EL, Buettner HM. Investigation of impinging-jet crystallization with a calcium oxalate model system. *Aiche Journal*. 2003;49(9):2352-2362.

27. Careno S, Boutin O, Badens E. Drug recrystallization using supercritical anti-solvent (SAS) process with impinging jets: Effect of process parameters. *Journal of Crystal Growth*. 2012;342(1):34-41.
28. Mahajan AJ, Kirwan DJ. Micromixing effects in a two-impinging-jets precipitator. *Aiche Journal*. 1996;42(7):1801-1814.
29. Woo XY, Tan RBH, Braatz RD. Precise tailoring of the crystal size distribution by controlled growth and continuous seeding from impinging jet crystallizers. *Crystengcomm*. 2011;13(6):2006-2014.
30. Woo XY, Tan RBH, Braatz RD. Modeling and computational fluid dynamics-population balance equation-micromixing simulation of impinging jet crystallizers. *Crystal Growth & Design*. 2009;9(1):156-164.
31. Jiang M, Wong MH, Zhu Z, et al. Towards achieving a flattop crystal size distribution by continuous seeding and controlled growth. *Chemical Engineering Science*. 2012;77:2-9.
32. Gower PE, Dash CH. Pharmacokinetics of cefuroxime after intravenous-injection. *European Journal of Clinical Pharmacology*. 1977;12(3):221-227.
33. Greenwood D, Pearson NJ, O'Grady F. Cefuroxime a new cephalosporin antibiotic with enhanced stability to enterobacterial beta lactamases. *Journal of Antimicrobial Chemotherapy*. 1976;2(4):337-343.
34. Fu GQ, Zhou ZJ, Dong QB, Long. WG, Inventors. Preparation of cefuroxime sodium. CN 101906109 A. 2010.
35. Liu WJ, Ma CY, Feng SX, Wang XZ. Solubility measurement and stability study of sodium cefuroxime. *Journal of Chemical & Engineering Data*. 2014;59(3):807-816.
36. Yu LX, Lionberger RA, Raw AS, D'Costa R, Wu HQ, Hussain AS. Applications of process analytical technology to crystallization processes. *Advanced Drug Delivery Reviews*. 2004;56(3):349-369.
37. Saleemi AN, Rielly CD, Nagy ZK. Monitoring of the combined cooling and antisolvent crystallisation of mixtures of aminobenzoic acid isomers using ATR-UV/vis spectroscopy and FBRM. *Chemical Engineering Science*. 2012;77:122-129.
38. Groen H, Roberts KJ. Application of ATR-FTIR spectroscopy for on-line determination of solute concentration and solution supersaturation. Paper presented at: Proceedings of the 14th international symposium on industrial crystallization. 1999. Cambridge.
39. Doki N, Yokota M, Sasaki S, Kubota N. Simultaneous crystallization of D- and L-asparagines in the presence of a tailor-made additive by natural cooling combined with pulse heating. *Crystal Growth & Design*. 2004;4(6):1359-1363.
40. Saleemi AN, Rielly CD, Nagy ZK. Comparative investigation of supersaturation and automated direct nucleation control of crystal size distributions using ATR-UV/vis spectroscopy and FBRM. *Crystal Growth & Design*. 2012;12(4):1792-1807.
41. Beggs HD, Parker JD. Determination of pressure drop optimum pipe size for 2 phase slug flow in an inclined pipe. *Journal of Engineering for Industry*. 1971;93(2):763-&.

42. Thompson E, Baalham CJ, Inventors; Glaxo Group Limited, England, assignee. Preparation of sodium cefuroxime. US 4,277,601. 1981.
43. Inoue M, Shima K, Inazu K. Crystal-growth of cephalothin sodium in frozen solution .2. effects of amount of seed, concentration, and temperature. *Yakugaku Zasshi-Journal of the Pharmaceutical Society of Japan.*1984;104(12):1268-1274.
44. Barrett P, Glennon B. In-line FBRM monitoring of particle size in dilute agitated suspensions. *Particle & Particle Systems Characterization.*1999;16(5):207-211.
45. Heath AR, Fawell PD, Bahri PA, Swift JD. Estimating average particle size by focused beam reflectance measurement (FBRM). *Particle & Particle Systems Characterization.* 2002;19(2):84-95.
46. Choo YJ, Kang BS. The effect of jet velocity profile on the characteristics of thickness and velocity of the liquid sheet formed by two impinging jets. *Physics of Fluids.* 2007;19(11).
47. Dehkordi AM, Safari I, Ebrahimi AA. Solid-Liquid Catalytic Reactions in a New Two-Impinging-Jets Reactor: Experiment and Modeling. *Industrial & Engineering Chemistry Research.* 2009;48(6):2861-2869.
48. Li R, Ashgriz N. Edge instability and velocity of liquid sheets formed by two impinging jets. *Atomization and Sprays.* 2007;17(1):71-97.
49. Saien J, Moradi V. Low interfacial tension liquid-liquid extraction with impinging-jets contacting method: Influencing parameters and relationship. *Journal of Industrial and Engineering Chemistry.* 2012;18(4):1293-1300.
50. Dehkordi AM, Ebrahimi AA. Catalytic Wet Peroxide Oxidation of Phenol in a New Two-Impinging-Jets Reactor. *Industrial & Engineering Chemistry Research.* 2009;48(23):10619-10626.
51. Kossel W. The energetics of surface procedures. *Annalen Der Physik.*1934;21(5):457-480.
52. Morgan N, Wells C, Kraft M, Wagner W. Modelling nanoparticle dynamics: coagulation, sintering, particle inception and surface growth. *Combustion Theory and Modelling.* 2005;9(3):449-461.

List of Figure Captions

Figure 1. The 1L rig that was used for both seeds preparation and reactive crystallization processes (A solvent mixture of ethanol and acetone (the same ratio with the reactants) was added into the tank reactor with/without seeds in order to submerge the nozzles of the impinging jet mixer in reactive crystallization process).

Figure 2. The 10L rig: (a) the schematic diagram (1 – the sodium lactate solution feed; 2 – the acid cefuroxime solution feed; 3 – the IKA EUROSTAR digital stirrer; 4 – the 10L tank reactor with a jacket; 5 – the impinging jet mixer); (b) the impinging jet mixer. (A solvent mixture of ethanol and acetone (the same ratio with the reactants) was added into the tank reactor with/without seeds in order to submerge the nozzles of the impinging jet mixer in reactive crystallization process).

Figure 3. The XRD spectra of sodium cefuroxime obtained from the 1L crystallizer (peak intensity and peak width at half height of peak between 9° to 10.5° were chosen to present the crystallinity): (a) The XRD spectra of sodium cefuroxime obtained from the 1L crystallizer for determination of the reaction temperature; (b) The XRD spectra of sodium cefuroxime obtained from the 1L crystallizer for determination of the feed rate; (c) The XRD spectra of sodium cefuroxime obtained from the 1L crystallizer for determination of the stirring speed. (the meaning of the monogram in the label table on the right side can be seen in Table 1, e.g. AEIN means the reaction temperature is 20°C (A), the feed rate is $2\text{ mL}\cdot\text{min}^{-1}$ (E), the stirring speed is 80 rpm (I) and the amount of seeds is 0.03 g (N)).

Figure 4. The Morphologi G3 results of sodium cefuroxime obtained from the 1L crystallizer for determination of the stirring speed during the optimization of reactive crystallization process (From left to right: Dark blue: BFLN (200 rpm); Green: BFKN (150 rpm); Light blue: BFJN (100 rpm); Brown: BFIN (80 rpm)).

Figure 5. The FBRM results of 1L un-seeded experiments for determination of the seed loading (the range of sizes for the FBRM counts is μm): (a) 20120523: $4 \text{ mL}\cdot\text{min}^{-1}$ (slower initial feed rate, the feed pump was opened one minute in every five minutes) + $4 \text{ mL}\cdot\text{min}^{-1}$ (the following continuous feed rate used when the feeding amount reached 40 mL - 70 mL); (b) 20120524: $10 \text{ mL}\cdot\text{min}^{-1}$ (faster initial feed rate, the feed pump was opened one minute in every five minutes) + $4 \text{ mL}\cdot\text{min}^{-1}$ (the following continuous feed rate used when the feeding amount reached 40 mL - 70 mL); (c) two repeat experiments following the same conditions with 20120523 and 20120524, respectively (The other operating conditions: temperature: 20 - 25 °C; stirring speed: 80 - 100 rpm; without impinging jet mixer; the feed rate was changed only in the experiments for the determination of the seed loading).

Figure 6. The XRD spectra of 1L un-seeded experiments for determination of the seed loading during the optimization of reactive crystallization process (peak intensity and peak width at half height of peak between 9° to 10.5° were chosen to present the crystallinity): black – 20120523: $4 \text{ mL}\cdot\text{min}^{-1}$ (slower initial feed rate, the feed pump was opened one minute in every five minutes) + $4 \text{ mL}\cdot\text{min}^{-1}$ (the following continuous feed rate used when the feeding amount reached 40 mL - 70 mL); red – 20120524: $10 \text{ mL}\cdot\text{min}^{-1}$ (faster initial feed rate, the feed pump was opened one minute in every five minutes) + $4 \text{ mL}\cdot\text{min}^{-1}$ (the following continuous feed rate used when the feeding amount reached 40 mL - 70 mL) (The other operating conditions: temperature: 20 - 25 °C; stirring speed: 80 - 100 rpm; without impinging jet mixer; the feed rate was changed only in the experiments for the determination of the seed loading).

Figure 7. The FBRM results of two 1L seeded reactive crystallization processes comparing with 20120524 ($10 \text{ mL}\cdot\text{min}^{-1}$ (faster initial feed rate, the feed pump was opened one minute in every five minutes) + $4 \text{ mL}\cdot\text{min}^{-1}$ (the following continuous feed rate used when the feeding amount reached 40

mL - 70 mL), un-seeded experiment) for determination of the seed loading during the optimization of reactive crystallization process (The other operating conditions: temperature: 20 - 25 °C; stirring speed: 80 - 100 rpm; without impinging jet mixer; the feed rate was changed only in the experiments for the determination of the seed loading).

Figure 8. The XRD spectra of sodium cefuroxime obtained from the 1L crystallizer for design of the impinging jet mixer (peak intensity and peak width at half height of peak between 9° to 10.5° were chosen to present the crystallinity): (a) 10° upward jets; (b) Parallel jets; (c) 10° downward jets. (the meaning of the monogram in the label table on the right side can be seen in Table 2, e.g. ADGH means the angel of the nozzles is 10° upward (A), the spacing between the two nozzles is 6.87 mm (D), the amount of seeds is 0.407 g (G), and the feed speed is 10 m·s⁻¹ (H)) (The other operating conditions: temperature: 20 - 25 °C; stirring speed: 80 - 100 rpm).

Figure 9. The XRD spectra of sodium cefuroxime obtained from the 1L crystallizer with/without the impinging jet mixer (peak intensity and peak width at half height of peak between 9° to 10.5° were chosen to present the crystallinity) (The other operating conditions: temperature: 20 - 25 °C; feed rate: 4 mL·min⁻¹ for acid cefuroxime solution and 1 mL·min⁻¹ for sodium lactate solution; stirring speed: 80 - 100 rpm; seeds: 0.407 g; feed speed: 10 m·s⁻¹).

Figure 10. The Morphologi G3 results of sodium cefuroxime obtained from the 1L crystallizer with/without the impinging jet mixer (From left to right: Green: 1L without impinging jet mixer; Brown: 1L with impinging jet mixer; Light blue: re-1L with impinging jet mixer-1; Dark blue: re-1L with impinging jet mixer-2) (The other operating conditions: temperature: 20 - 25 °C; feed rate: 4 mL·min⁻¹ for acid cefuroxime solution and 1 mL·min⁻¹ for sodium lactate solution; stirring speed: 80 - 100 rpm; seeds: 0.407 g; feed speed: 10 m·s⁻¹).

Figure 11. The XRD spectra of sodium cefuroxime obtained from the 10L crystallizer with/without the impinging jet mixer (peak intensity and peak width at half height of peak between 9° to 10.5°

were chosen to present the crystallinity). (The other operating conditions: temperature: 20 - 25 °C; feed rate: 40 mL·min⁻¹ for acid cefuroxime solution and 10 mL·min⁻¹ for sodium lactate solution; seeds: 4.07 g; feed speed: 10 m·s⁻¹).

Figure 12. The Morphologi G3 results of sodium cefuroxime obtained from the 10L crystallizer with/without the impinging jet mixer (From left to right: Green: 10L without impinging jet mixer-50 rpm; Dark blue: 10L with impinging jet mixer-80 rpm; Light blue: 10L with impinging jet mixer-50 rpm; Brown: re-10L with impinging jet mixer-50 rpm) (The other operating conditions: temperature: 20 - 25 °C; feed rate: 40 mL·min⁻¹ for acid cefuroxime solution and 10 mL·min⁻¹ for sodium lactate solution; seeds: 4.07 g; feed speed: 10 m·s⁻¹).

Figure 13. The SEM images of sodium cefuroxime obtained from the 10L impinging jet mixer scale-up experiments: (a) 10L without impinging jet mixer-50 rpm; (b) 10L with impinging jet mixer-50 rpm; (c) the seeds.

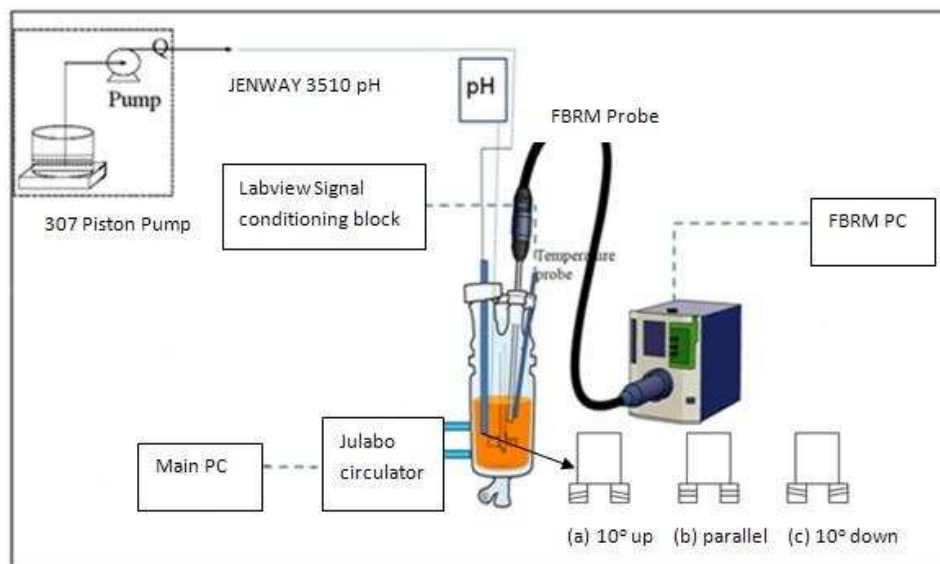
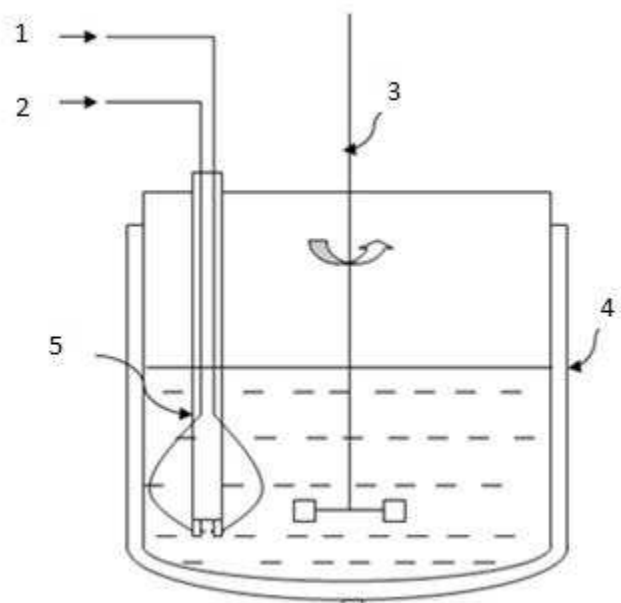


Figure 1. The 1L rig that was used for both seeds preparation and reactive crystallization processes (A solvent mixture of ethanol and acetone (the same ratio with the reactants) was added into the tank reactor with/without seeds in order to submerge the nozzles of the impinging jet mixer in reactive crystallization process).

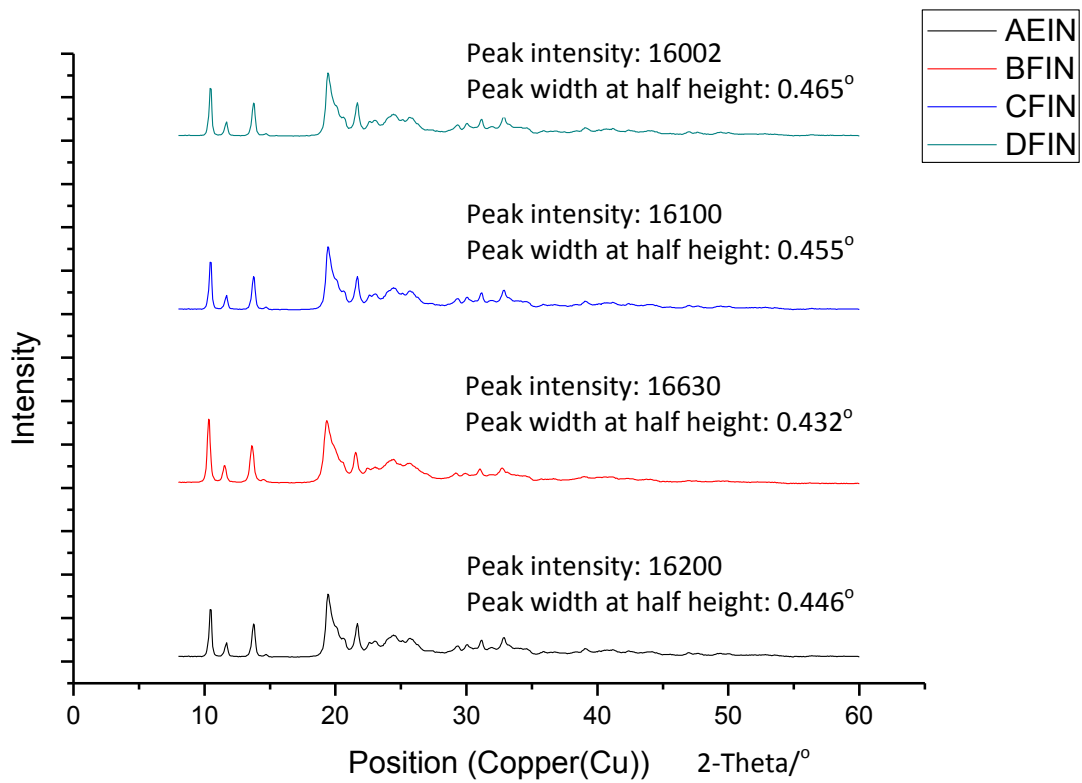


(a)

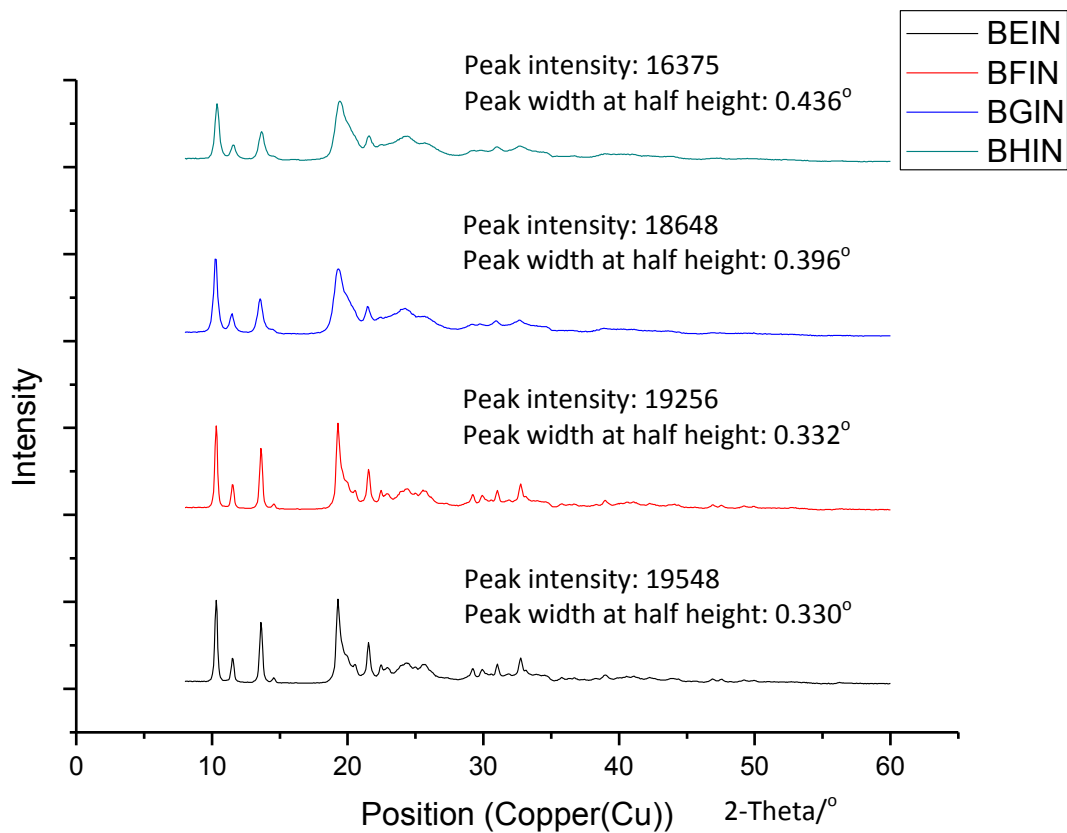


(b)

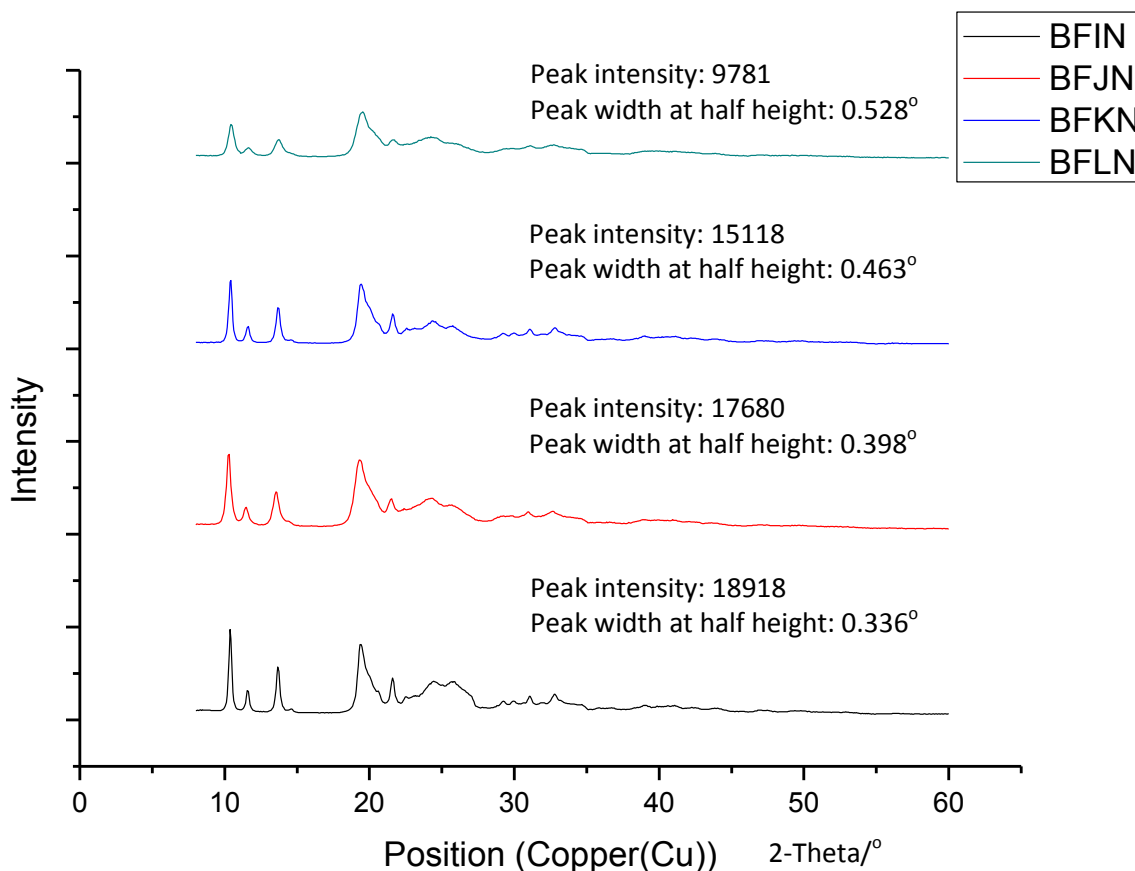
Figure 2. The 10L rig: (a) the schematic diagram (1 – the sodium lactate solution feed; 2 – the acid cefuroxime solution feed; 3 – the IKA EUROSTAR digital stirrer; 4 – the 10L tank reactor with a jacket; 5 – the impinging jet mixer); (b) the impinging jet mixer. (A solvent mixture of ethanol and acetone (the same ratio with the reactants) was added into the tank reactor with/without seeds in order to submerge the nozzles of the impinging jet mixer in reactive crystallization process).



(a)



(b)



(c)

Figure 3. The XRD spectra of sodium cefuroxime obtained from the 1L crystallizer (peak intensity and peak width at half height of peak between 9° to 10.5° were chosen to present the crystallinity): (a) The XRD spectra of sodium cefuroxime obtained from the 1L crystallizer for determination of the reaction temperature; (b) The XRD spectra of sodium cefuroxime obtained from the 1L crystallizer for determination of the feed rate; (c) The XRD spectra of sodium cefuroxime obtained from the 1L crystallizer for determination of the stirring speed. (the meaning of the monogram in the label table on the right side can be seen in Table 1, e.g. AEIN means the reaction temperature is 20°C (A), the feed rate is $2\text{ mL}\cdot\text{min}^{-1}$ (E), the stirring speed is 80 rpm (I) and the amount of seeds is 0.03 g (N)).

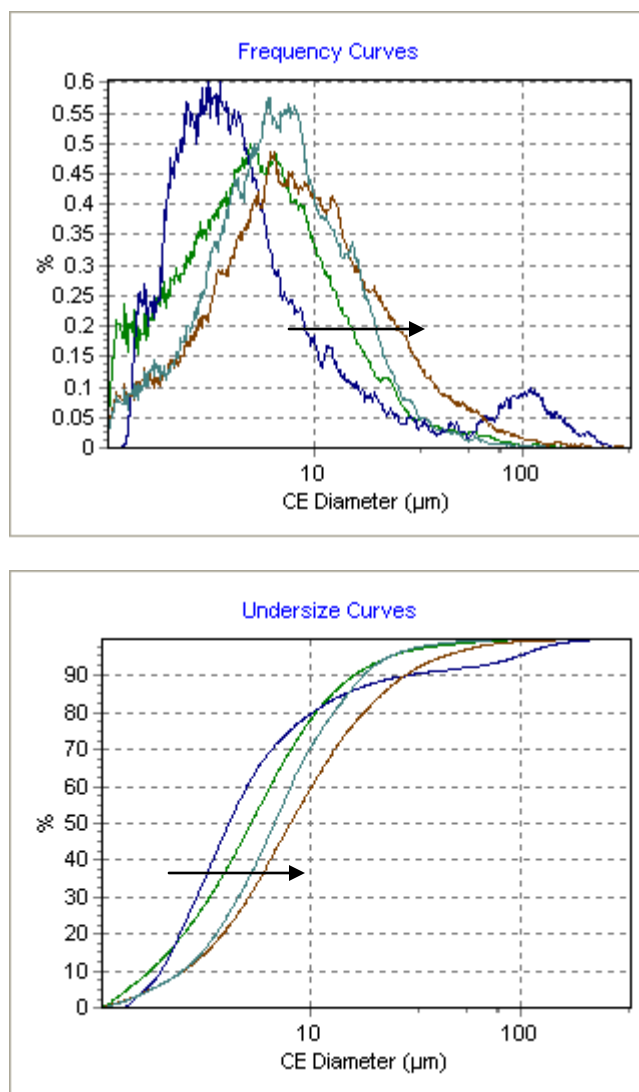
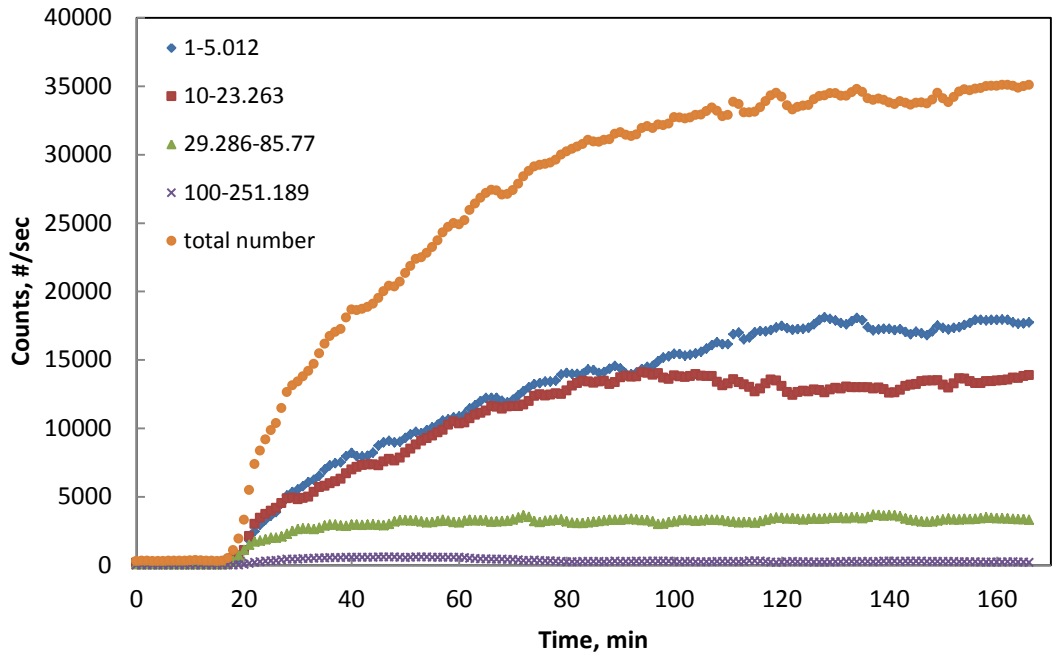
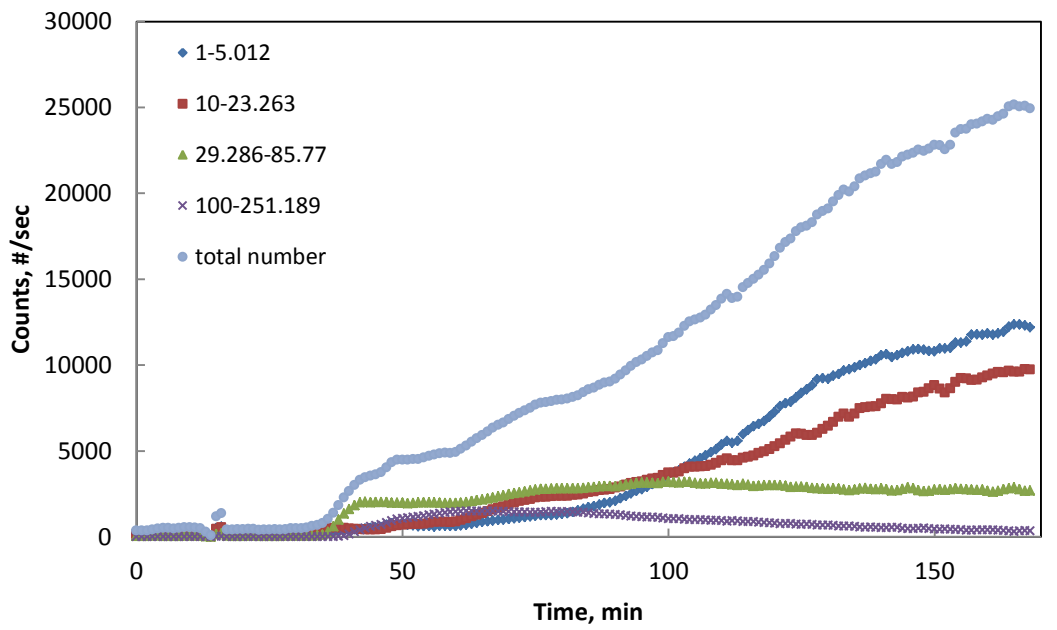


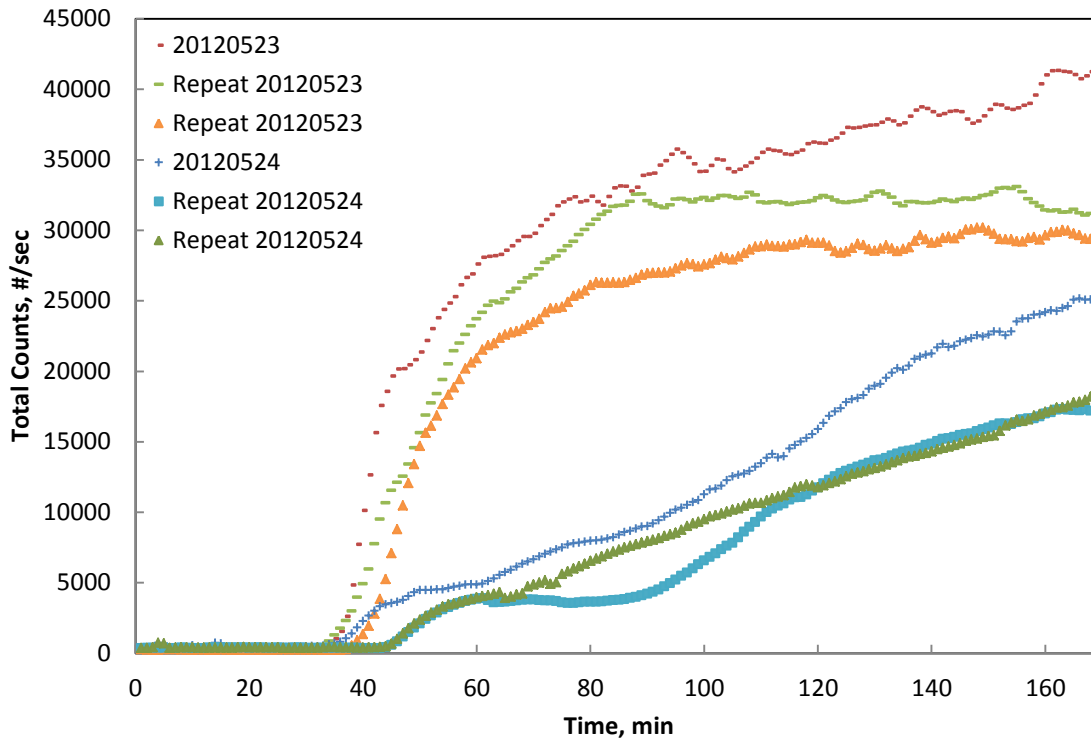
Figure 4. The Morphologi G3 results of sodium cefuroxime obtained from the 1L crystallizer for determination of the stirring speed during the optimization of reactive crystallization process (From left to right: Dark blue: BFLN (200 rpm); Green: BFKN (150 rpm); Light blue: BFJN (100 rpm); Brown: BFIN (80 rpm)).



(a)



(b)



(c)

Figure 5. The FBRM results of 1L un-seeded experiments for determination of the seed loading (the range of sizes for the FBRM counts is μm): (a) 20120523: $4 \text{ mL}\cdot\text{min}^{-1}$ (slower initial feed rate, the feed pump was opened one minute in every five minutes) + $4 \text{ mL}\cdot\text{min}^{-1}$ (the following continuous feed rate used when the feeding amount reached 40 mL - 70 mL); (b) 20120524: $10 \text{ mL}\cdot\text{min}^{-1}$ (faster initial feed rate, the feed pump was opened one minute in every five minutes) + $4 \text{ mL}\cdot\text{min}^{-1}$ (the following continuous feed rate used when the feeding amount reached 40 mL - 70 mL); (c) two repeat experiments following the same conditions with 20120523 and 20120524, respectively (The other operating conditions: temperature: 20 - 25 °C; stirring speed: 80 - 100 rpm; without impinging jet mixer; the feed rate was changed only in the experiments for the determination of the seed loading).

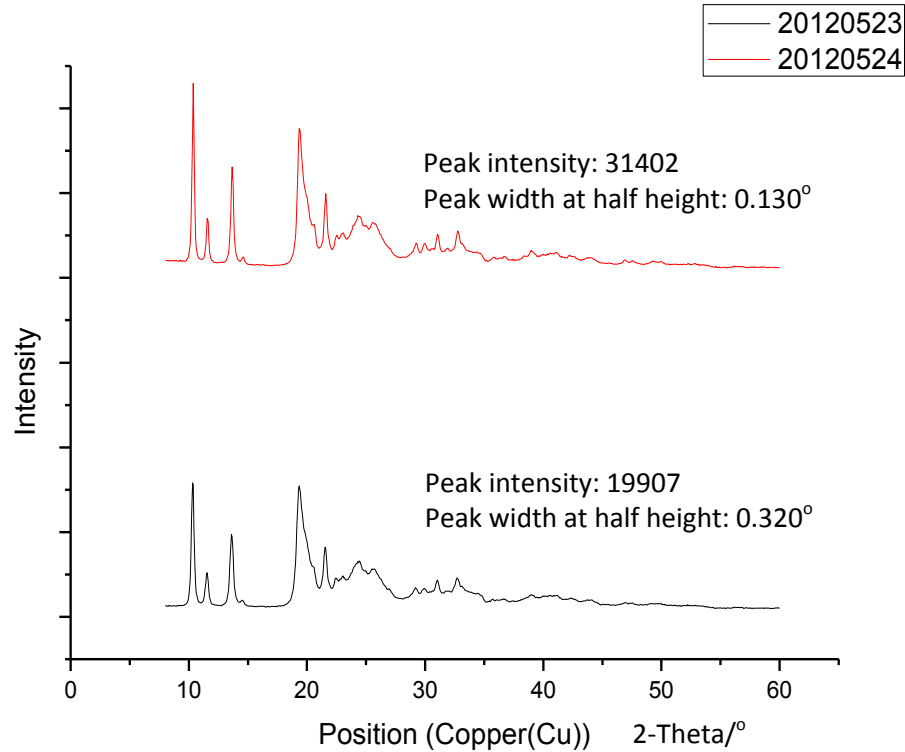


Figure 6. The XRD spectra of 1L un-seeded experiments for determination of the seed loading during the optimization of reactive crystallization process (peak intensity and peak width at half height of peak between 9° to 10.5° were chosen to present the crystallinity): black – 20120523: $4 \text{ mL}\cdot\text{min}^{-1}$ (slower initial feed rate, the feed pump was opened one minute in every five minutes) + $4 \text{ mL}\cdot\text{min}^{-1}$ (the following continuous feed rate used when the feeding amount reached 40 mL - 70 mL); red – 20120524: $10 \text{ mL}\cdot\text{min}^{-1}$ (faster initial feed rate, the feed pump was opened one minute in every five minutes) + $4 \text{ mL}\cdot\text{min}^{-1}$ (the following continuous feed rate used when the feeding amount reached 40 mL - 70 mL) (The other operating conditions: temperature: 20 - 25 °C; stirring speed: 80 - 100 rpm; without impinging jet mixer; the feed rate was changed only in the experiments for the determination of the seed loading).

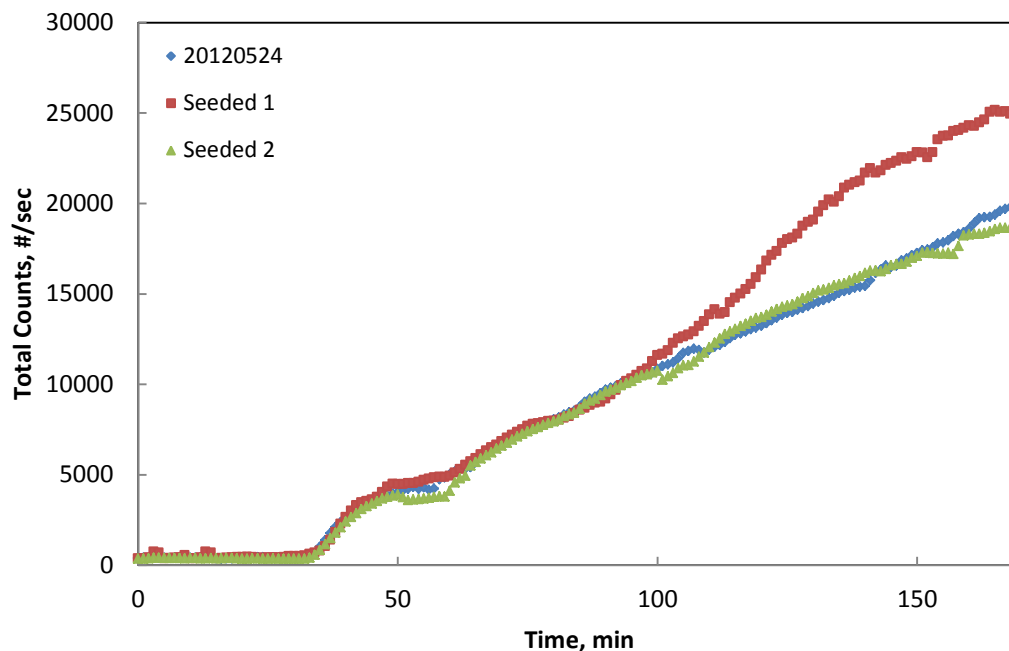
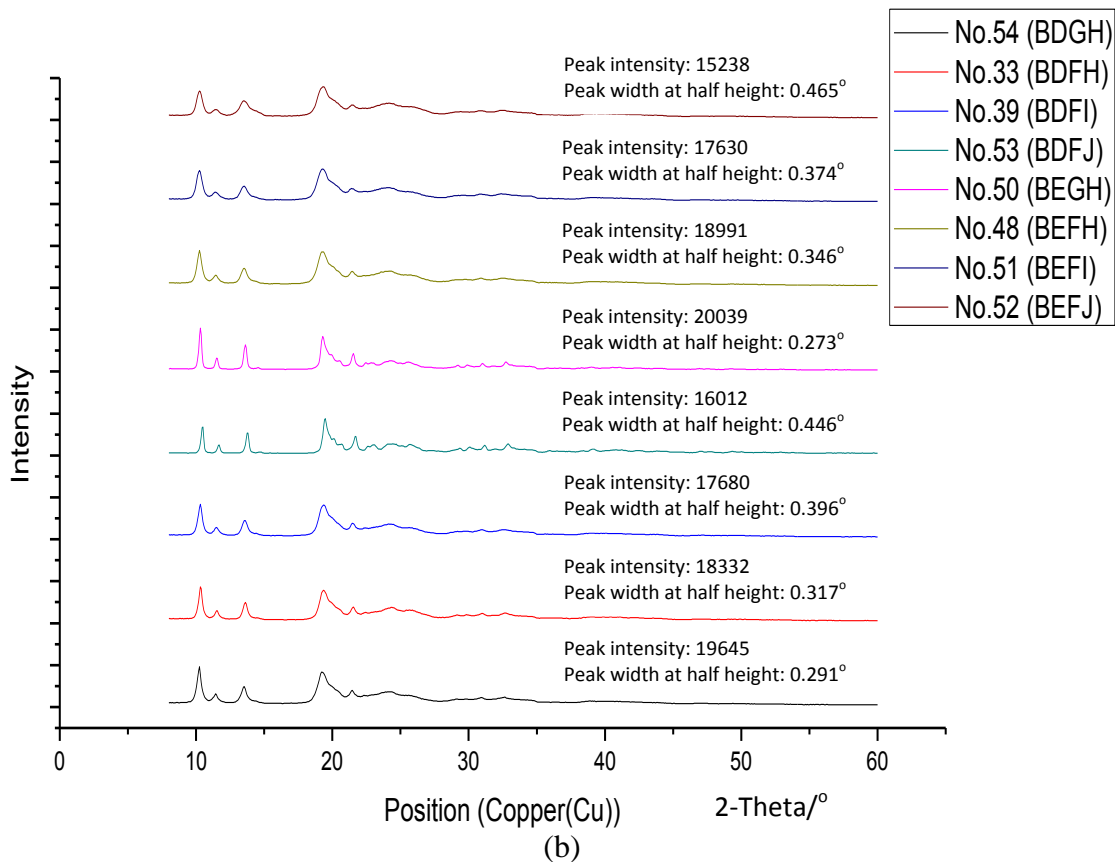
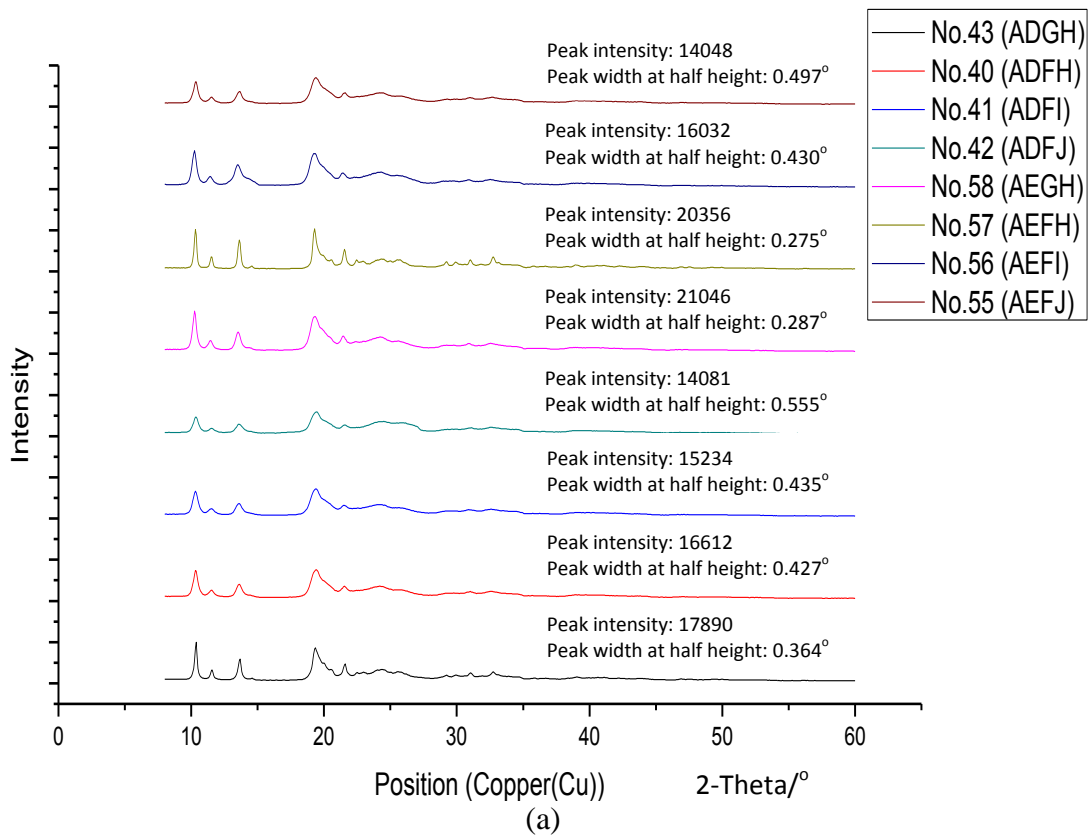
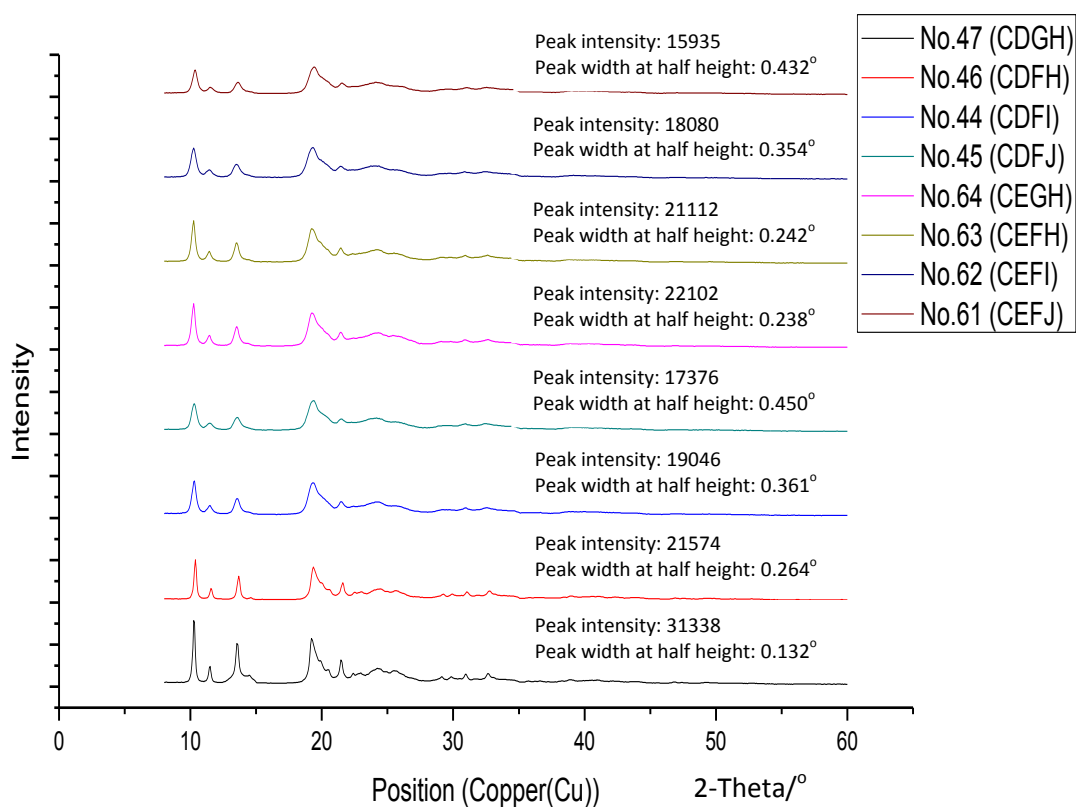


Figure 7. The FBRM results of two 1L seeded reactive crystallization processes comparing with 20120524 ($10 \text{ mL} \cdot \text{min}^{-1}$ (faster initial feed rate, the feed pump was opened one minute in every five minutes) + $4 \text{ mL} \cdot \text{min}^{-1}$ (the following continuous feed rate used when the feeding amount reached 40 mL - 70 mL), un-seeded experiment) for determination of the seed loading during the optimization of reactive crystallization process (The other operating conditions: temperature: 20 - 25 °C; stirring speed: 80 - 100 rpm; without impinging jet mixer; the feed rate was changed only in the experiments for the determination of the seed loading).





(c)

Figure 8. The XRD spectra of sodium cefuroxime obtained from the 1L crystallizer for design of the impinging jet mixer (peak intensity and peak width at half height of peak between 9° to 10.5° were chosen to present the crystallinity): (a) 10° upward jets; (b) Parallel jets; (c) 10° downward jets. (the meaning of the monogram in the label table on the right side can be seen in Table 2, e.g. ADGH means the angel of the nozzles is 10° upward (A), the spacing between the two nozzles is 6.87 mm (D), the amount of seeds is 0.407 g (G), and the feed speed is $10 \text{ m}\cdot\text{s}^{-1}$ (H)) (The other operating conditions: temperature: $20 - 25^\circ\text{C}$; stirring speed: 80 - 100 rpm).

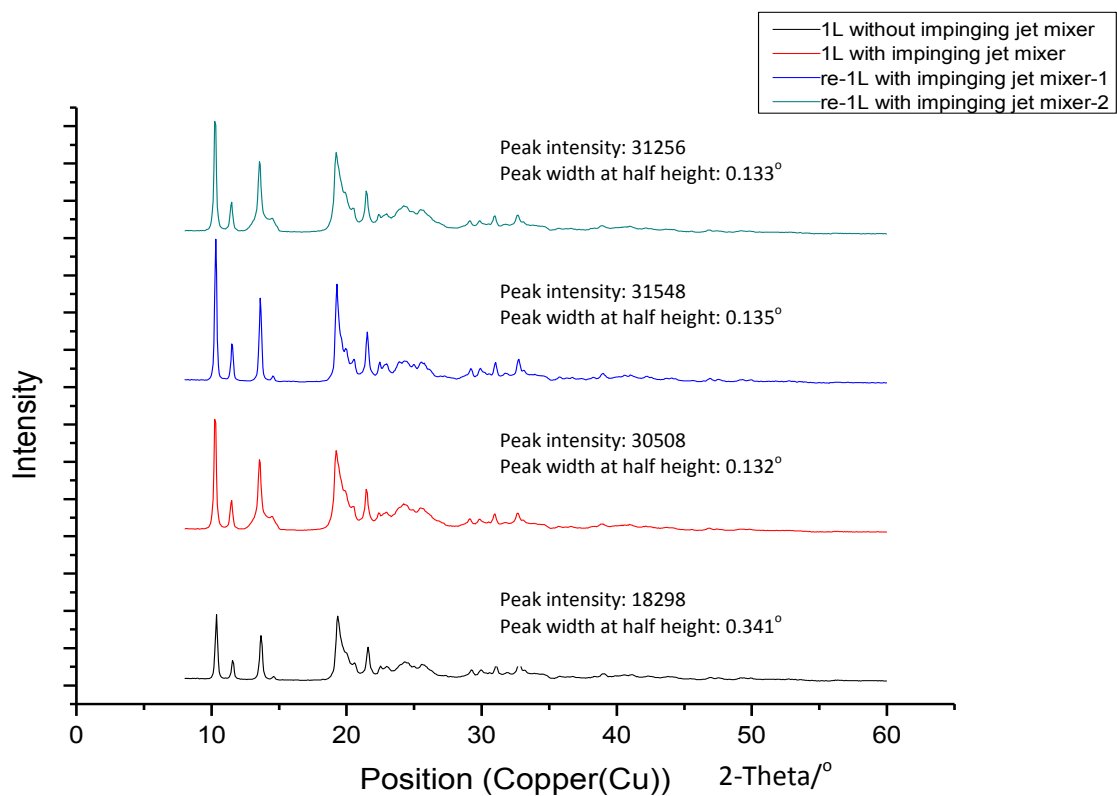


Figure 9. The XRD spectra of sodium cefuroxime obtained from the 1L crystallizer with/without the impinging jet mixer (peak intensity and peak width at half height of peak between 9° to 10.5° were chosen to present the crystallinity) (The other operating conditions: temperature: $20 - 25^{\circ}\text{C}$; feed rate: $4\text{ mL}\cdot\text{min}^{-1}$ for acid cefuroxime solution and $1\text{ mL}\cdot\text{min}^{-1}$ for sodium lactate solution; stirring speed: $80 - 100\text{ rpm}$; seeds: 0.407 g ; feed speed: $10\text{ m}\cdot\text{s}^{-1}$).

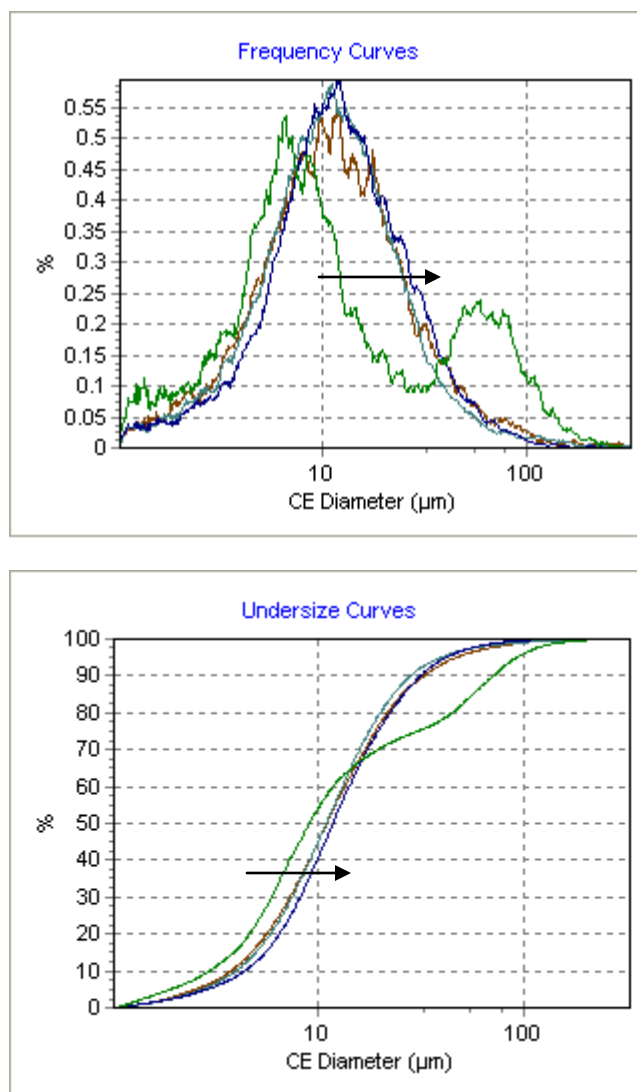


Figure 10. The Morphologi G3 results of sodium cefuroxime obtained from obtained from the 1L crystallizer with/without the impinging jet mixer (From left to right: Green: 1L without impinging jet mixer; Brown: 1L with impinging jet mixer; Light blue: re-1L with impinging jet mixer-1; Dark blue: re-1L with impinging jet mixer-2) (The other operating conditions: temperature: 20 - 25 °C; feed rate: 4 mL·min⁻¹ for acid cefuroxime solution and 1 mL·min⁻¹ for sodium lactate solution; stirring speed: 80 - 100 rpm; seeds: 0.407 g; feed speed: 10 m·s⁻¹).

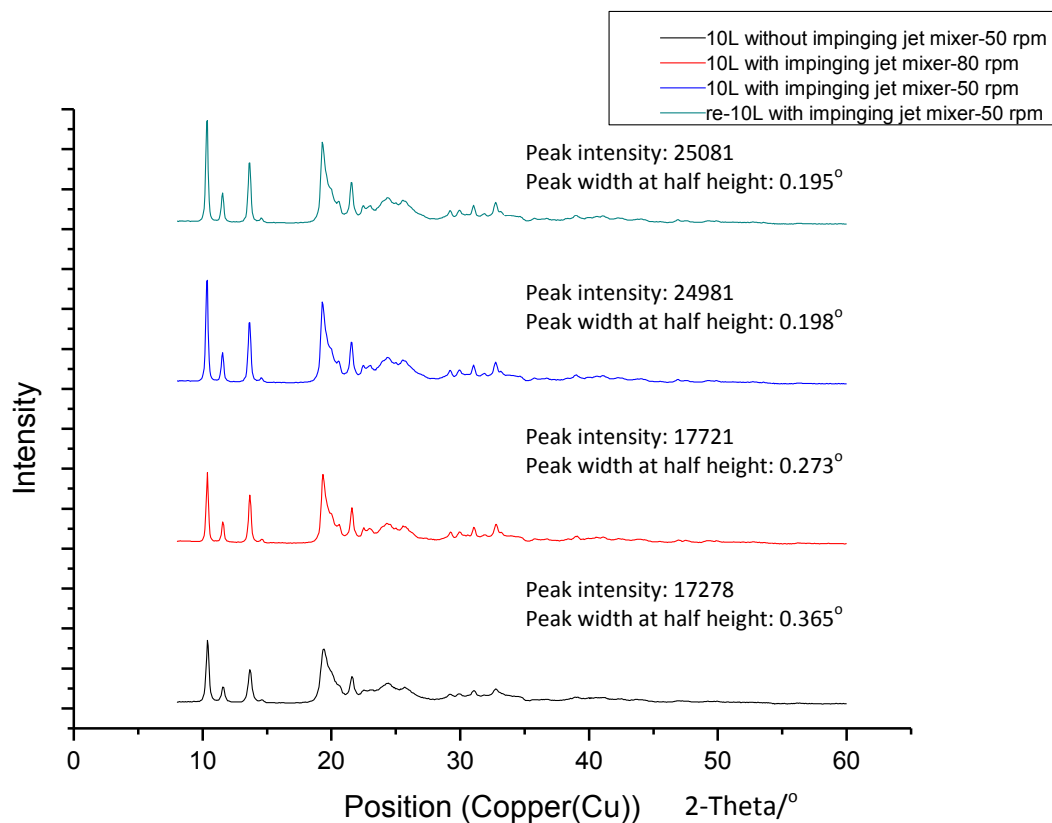


Figure 11. The XRD spectra of sodium cefuroxime obtained from the 10L crystallizer with/without the impinging jet mixer (peak intensity and peak width at half height of peak between 9° to 10.5° were chosen to present the crystallinity). (The other operating conditions: temperature: $20 - 25^{\circ}\text{C}$; feed rate: $40 \text{ mL}\cdot\text{min}^{-1}$ for acid cefuroxime solution and $10 \text{ mL}\cdot\text{min}^{-1}$ for sodium lactate solution; seeds: 4.07 g ; feed speed: $10 \text{ m}\cdot\text{s}^{-1}$).

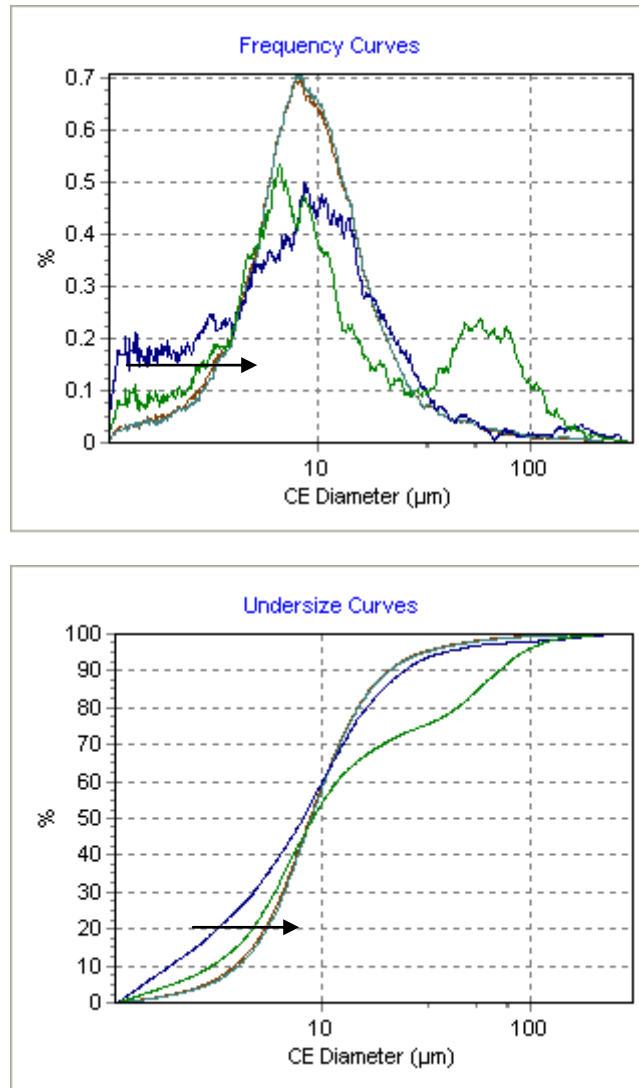
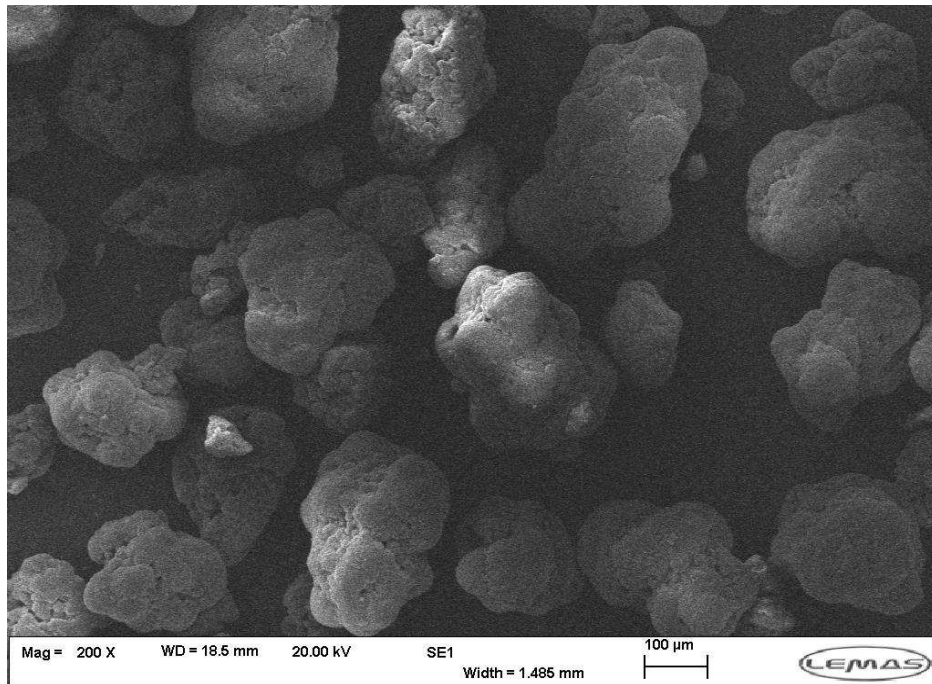
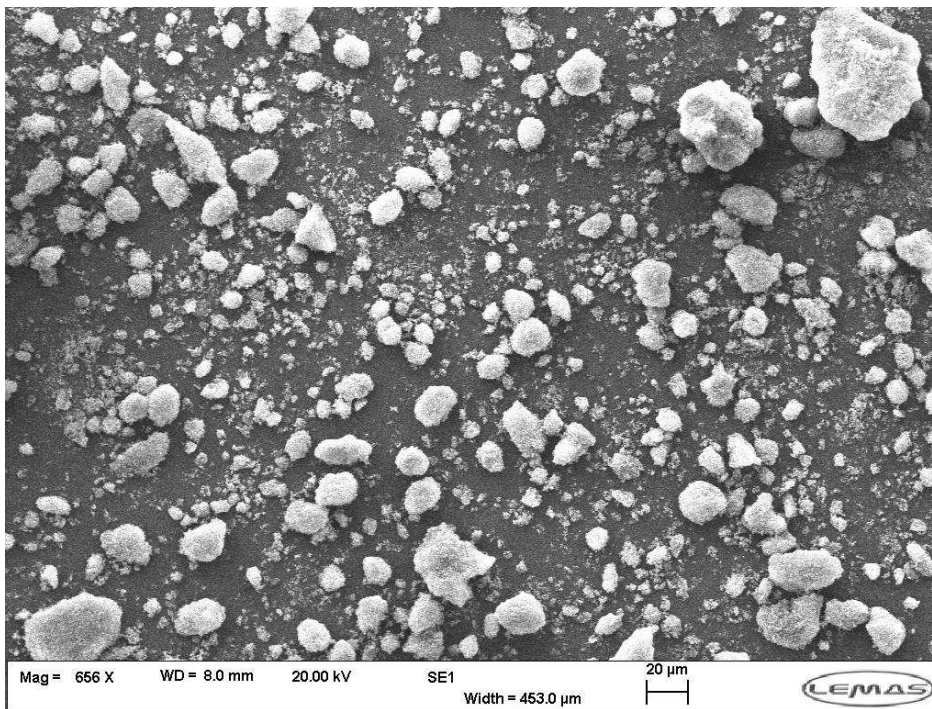


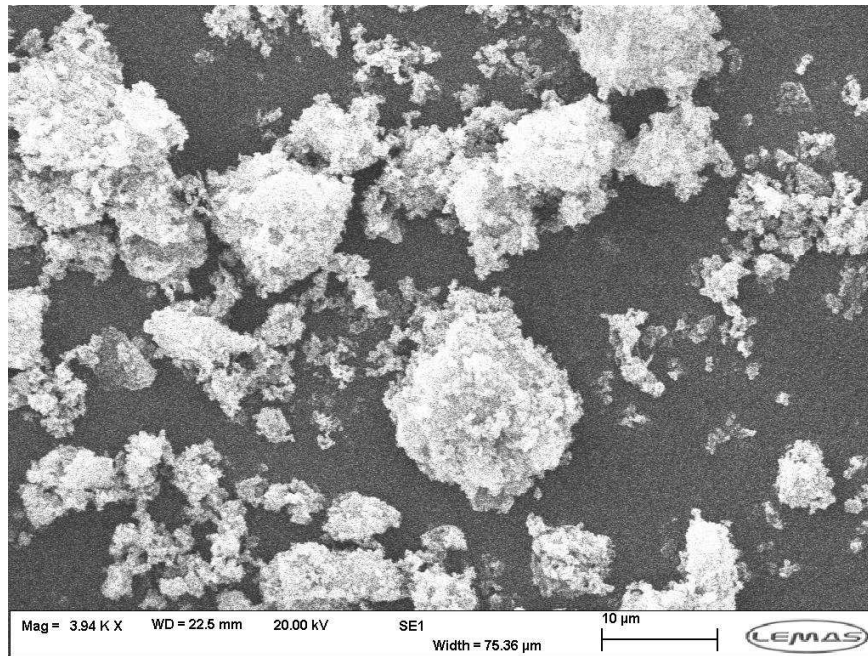
Figure 12. The Morphologi G3 results of sodium cefuroxime obtained from the 10L crystallizer with/without the impinging jet mixer (From left to right: Green: 10L without impinging jet mixer-50 rpm; Dark blue: 10L with impinging jet mixer-80 rpm; Light blue: 10L with impinging jet mixer-50 rpm; Brown: re-10L with impinging jet mixer-50 rpm) (The other operating conditions: temperature: 20 - 25 °C; feed rate: 40 mL·min⁻¹ for acid cefuroxime solution and 10 mL·min⁻¹ for sodium lactate solution; seeds: 4.07 g; feed speed: 10 m·s⁻¹).



(a)



(b)



(c)

Figure 13. The SEM images of sodium cefuroxime obtained from the 10L impinging jet mixer scale-up experiments: (a) 10L without impinging jet mixer-50 rpm; (b) 10L with impinging jet mixer-50 rpm; (c) the seeds.

Table 1. Operation Parameters of the Optimization Experiments in the 1L Crystallizer without the Impinging Jet Mixer.*

Reaction temperature (°C)	Feed rate (mL·min ⁻¹)	Stirring speed (rpm)	Amount of seeds (g)
20 (A)	2 (E)	80 (I)	None (M)
25 (B)	4 (F)	100 (J)	0.03 (N)
30 (C)	6 (G)	150 (K)	
35 (D)	8 (H)	200 (L)	

* The letters A B and C were used in Figure 3 and Figure 4 to denote the operating conditions.

Table 2. Design Parameters of the Impinging Jet Mixers. *

Angle	Spacing (mm)	Amount of Seed (g)	Feed Speed ($\text{m}\cdot\text{s}^{-1}$)
10° Upward (A)	6.87 (D)	None (F)	10 (H)
Parallel (B)	11.76 (E)	0.407g (G)	15 (I)
10° Downward (C)			20 (J)

*The letters A B and C were used in Figure 8 to denote the designs. The diameters of two nozzles were 0.13 mm and 0.065 mm in the 1L crystallizer, 0.3 mm and 0.15 mm in the 10L crystallizer.

Table 3. Analysis Result of Sodium Cefuroxime Obtained from the 1L Experiments.*

Batch No	Water Content (w/w %)	Colour Grade	Sodium Cefuroxime Content (HPLC) (w/w %)
1L without impinging jet mixer	2.12	<Y-2#	91.33
1L with impinging jet mixer	0.55	<Y-2#	94.91
re-1L with impinging jet mixer-1	0.59	<Y-2#	95.51
re-1L with impinging jet mixer-2	0.57	<Y-2#	95.36

* Y means the colour grade yellow. The other operating conditions: temperature: 20 - 25 °C; feed rate: 4 mL·min⁻¹ for acid cefuroxime solution and 1 mL·min⁻¹ for sodium lactate solution; stirring speed: 80 - 100 rpm; seeds: 0.407 g; feed speed: 10 m·s⁻¹.

Table 4. Stability Test Data of Sodium Cefuroxime Obtained from the 1L Experiments.*

Batch No	Color Grade (60°C)			
	0 day	3 days	5 days	7 days
1L without impinging jet mixer	<Y-2#	<Y-7#	<Y-9#	<Y-10#
1L with impinging jet mixer	<Y-2#	<Y-5#	<Y-7#	<Y-8#
re-1L with impinging jet mixer-1	<Y-2#	<Y-5#	<Y-7#	<Y-8#
re-1L with impinging jet mixer-2	<Y-2#	<Y-5#	<Y-6#	<Y-8#

* Y means the colour grade yellow. The other operating conditions: temperature: 20 - 25 °C; feed rate: 4 mL·min⁻¹ for acid cefuroxime solution and 1 mL·min⁻¹ for sodium lactate solution; stirring speed: 80 - 100 rpm; seeds: 0.407 g; feed speed: 10 m·s⁻¹.

Table 5. Analysis Result of Sodium Cefuroxime Obtained from the 10L Impinging Jet Mixer Scale-Up Experiments.*

Batch No	Water Content (w/w %)	Color Grade	Sodium Cefuroxime Content (HPLC) (w/w %)
10L without impinging jet mixer-50 rpm	2.22	<Y-2#	90.97
10L with impinging jet mixer-80 rpm	2.20	<Y-2#	94.43
10L with impinging jet mixer-50 rpm	0.60	<Y-2#	94.36
re-10L with impinging jet mixer-50 rpm	0.69	<Y-2#	93.19

* Y means the colour grade yellow. The other operating conditions: temperature: 20 - 25 °C; feed rate: 40 mL·min⁻¹ for acid cefuroxime solution and 10 mL·min⁻¹ for sodium lactate solution; seeds: 4.07 g; feed speed: 10 m·s⁻¹.

Table 6. Stability Test Data of Sodium Cefuroxime Obtained from the 10L Impinging Jet Mixer Scale-Up Experiments.*

Batch No	Color Grade (60°C)					Color Grade (40°C)	
	0 day	3 days	5 days	7 days	10 days	5 days	10 days
10L without impinging jet mixer-50 rpm	<Y-2#	<Y-9#	<Y-10#	>Y-10#	>Y-10#	<Y-3#	<Y-5#
10L with impinging jet mixer-80 rpm	<Y-2#	<Y-7#	<Y-8#	<Y-9#	<Y-9#	<Y-3#	<Y-4#
10L with impinging jet mixer-50 rpm	<Y-2#	<Y-7#	<Y-8#	<Y-8#	<Y-9#	<Y-3#	<Y-4#
re-10L with impinging jet mixer-50 rpm	<Y-2#	<Y-7#	<Y-8#	<Y-8#	<Y-9#	<Y-3#	<Y-4#

* Y means the colour grade yellow. The other operating conditions: temperature: 20 - 25 °C; feed rate: 40 mL·min⁻¹ for acid cefuroxime solution and 10 mL·min⁻¹ for sodium lactate solution; seeds: 4.07 g; feed speed: 10 m·s⁻¹.